tomography scans, preexisting chronic ILD, and concurrent cardiac diseases are known as risk factors for ILD in gefitinib treatment [10]. Although an assessment of pulmonary comorbidities, especially ILDs, is important to decrease the incidence of ILD induced by chemotherapy, the frequency of EGFR mutation in patients with pulmonary fibrosis and the clinical feature of these patients are not clear.

We reviewed 198 patients who were examined for EGFR mutation status and assessed the association of EGFR mutations with the underlying pulmonary diseases on chest high-resolution computed tomography (HRCT).

2. Methods

The medical records of a series of consecutive patients with histologically- or cytologically-proven lung cancer, who were tested for EGFR mutation status in the Division of Diagnostic Pathology, NTT Medical Center Tokyo between April 2008 and November 2010, were retrospectively reviewed. The status of EGFR mutation was examined in a clinical practice, not investigational setting, to decide the indication of EGFR-TKI treatment. Although most patients with severe pulmonary fibrosis or squamous cell carcinoma were excluded from the EGFR mutation test in this period, gender, smoking status, and the existence of emphysema were not considered as the exclusion criteria of the test. Patients with emphysema and fibrosis on chest HRCT at the diagnosis of lung cancer were prospectively identified, and the data before lung cancer treatment was recorded to assess their risk of ILD. Only patients who had a chest HRCT scan, which was performed at diagnosis of lung cancer and was available for review, were included in the study. The study protocol was reviewed and approved by the Ethics Committee of NTT Medical Center Tokyo.

Patients were categorized into three groups; those with normal lungs (except for the tumor), emphysematous lungs, or fibrotic lungs, based on chest CT findings as described previously [11, 12]. Patients who met the following criteria were categorized as having emphysema: the presence of emphysema on CT, defined as well-demarcated areas of decreased attenuation in comparison with contiguous normal lung, and marginated by a very thin (<1 mm) wall or no wall, and/or multiple bullae (>1 cm) with upper zone predominance. Patients who met the following criteria were categorized as having fibrosis: the presence of diffuse parenchymal lung disease with significant pulmonary fibrosis on CT, defined as reticular opacities with peripheral and basal predominance, honeycombing, architectural distortion, and/or traction bronchiectasis or bronchiolectasis; focal ground-glass opacities and/or areas of alveolar condensation may be associated, but should not be prominent. Patients who met neither criterion emphysema nor fibrosis were categorized as normal. The electronic medical records were reviewed to obtain clinical and demographic data, including gender, age, smoking history, histology results, clinical stage of lung cancer, treatment, treatment-related toxicities, and survival.

2.1. EGFR Mutation Analysis. The presence of EGFR mutations was determined by the peptide nucleic acid-locked nucleic acid PCR clamp method as described previously [13]. The investigated EGFR-TKI sensitive mutations included G719C, G719S, G719A, L858R, L861Q, and exon 19 deletions, as well as a gefitinib-resistant mutation, T790M.

2.2. Statistical Analysis. Differences among the categorized groups were compared using either the two-sided chi-square test or Fisher's exact test. The survival was estimated by the Kaplan-Meier method, and differences in survival between the subgroups were analyzed by the log rank test. Data were analyzed using the StatView version 5.0J software package (Statistical Analysis Systems, Cary, NC, USA).

3. Results

3.1. Subtypes of EGFR Mutations. We examined the EGFR mutation status in 202 patients between April 2008 and November 2010. We excluded 4 patients from this study for the following reasons: one had small cell lung cancer, two had gastric cancer, and one had parotid cancer. Of the 198 patients with nonsmall cell lung cancer, 52 patients (26.3%) had EGFR-TKI-sensitive EGFR mutations, and one patient had an EGFR-TKI-resistant mutation (T790M) with an EGFR-TKI-sensitive mutation (Exon 19 deletion). The patient population in this analysis (Table 1) was a little young, including more female, less never-smoker, and less squamous cell carcinoma of the lung in comparison with the lung cancer cohort that we previously published [12].

3.2. The Variables Associated with the EGFR Mutation Status. We investigated the association of several variables with the EGFR mutations (Table 2). A two-sided chi-square test showed that gender (female), smoking status (never smoker), histology (adenocarcinoma), and chest CT findings (normal) were significantly associated with the presence of an EGFR mutation. Of 122 patients with normal lungs, 69 patients had no history of smoking and 53 patients had a history of smoking. The frequency of EGFR mutations (n, %) in patients with normal lungs did not differ between smokers (17, 32.1%) and never-smokers (26, 37.7%) ($P = 0.5698$).

3.3. Prognosis of Patients with EGFR Mutations Treated with Gefitinib. All patients with an EGFR mutation were treated in the Division of Respirology and Chest Surgery, NTT Medical Center Tokyo. Of the 52 patients with EGFR mutation, 43 patients received gefitinib. The clinical characteristics of the patients with an EGFR mutation treated with gefitinib are shown in Table 3. The median survival after gefitinib treatment was 797 days. We identified ILD in two patients during gefitinib treatment; one had no ILD before gefitinib treatment and one had pulmonary fibrosis. The patient with pulmonary fibrosis developed acute exacerbation of preexisting ILD on day 7 of gefitinib treatment and died on day 14 because of ILD. The survival curves of the 42 patients, excluding the patient with pulmonary fibrosis, according to smoking status and chest CT results, are shown in Figures 1(a) and 1(b), respectively. No differences in survival were observed between smokers ($n = 18$, MST not reached) and never-smokers ($n = 24$, MST 797 days) or between

Table 1: Patient characteristics NSCLC: nonsmall cell lung cancer: LCNEC; large cell neuroendocrine carcinoma.

Total number of patients	198
Age (median, range)	68, 28–92
Gender	
Female	86
Male	112
Smoking-status	
Never	74
Ex/Current	124
Histology	
Adenocarcinoma	169
Squamous cell carcinoma	9
Other NSCLC	15
LCNEC	4
Clinical stage of NSCLC	
IA	29
IB	14
IIA	2
IIB	6
IIIA	12
IIIB	30
IV	105
Chest CT	
Normal	122
Emphysema	59
Fibrosis	17
EGFR mutation	
Wild type	147
Ex18 G718S	1
Ex19 del	34
Ex21 L858R	15
EX19 del + Ex21 L858R	1
Ex 19del + T790M	1

Table 2: Patient characteristics and EGFR mutation status.

	Number	EGFR mutation (n, %)	P-value
Gender			
Male	112	17, 15.2%	$P < 0.0001$
Female	86	35, 40.7%	
Age			
<65	80	23, 28.8%	$P = 0.5156$
65≤	118	29, 24.6%	
Histology			
Adenocarcinoma	169	50, 29.6%	$P = 0.0107$
Nonadenocarcinoma	29	2, 6.9%	
Smoking status			
Never	74	29, 39.2%	$P = 0.0139$
Ex/Current	124	23, 18.5%	
Clinical stage of NSCLC			
I-IIIA	63	21, 33.3%	$P = 0.1649$
IIIB-IV	135	31, 22.9%	
Chest CT			
Normal	122	43, 35.2%	
Emphysema	59	8, 13.6%	$P = 0.0011$
Fibrosis	17	1, 5.8%	

patients with normal lung (n = 36, MST 874 days) and those with emphysematous lungs (n = 6, MST 749 days) on chest CT.

4. Discussion

We herein showed the frequency of EGFR mutation in nonsmall cell lung cancer to be high in patients with the following factors: female gender, no history of smoking, adenocarcinoma, and normal lungs on chest CT. A survival analysis of the patients with EGFR mutations, excluding one patient with pulmonary fibrosis, showed no differences between smokers and never-smokers or between patients with emphysema and those with normal lungs on chest CT.

There is considerable variability in the susceptibility of smokers to developing smoking-related pulmonary diseases [14–16]. The incidence of lung cancer is increased in patients with emphysema and fibrosis, and this effect is independent of the effect of cigarette smoking [17, 18]. We consider that smokers with emphysema or fibrosis are more susceptible to smoking-related inflammation compared to those with normal lungs. Although the frequency of EGFR mutation was low in patients with emphysema and fibrosis, the frequency in those with normal lungs was not different between smokers and never-smokers. Our data suggested that smokers with normal lungs were not susceptible to smoking-related inflammation, and that nonsmall cell lung cancer in smokers with normal lungs showed the same biological features to that in never-smokers. Further investigations are necessary to elucidate whether smoking-related pulmonary diseases and lung cancer might result from overlapping or associated genetic variants implicated in smoking-related inflammation.

Although a history of smoking and the coexistence of emphysema were negatively associated with the frequency of EGFR mutations, these clinical factors did not affect the prognosis of the patients with EGFR mutations treated with gefitinib. Toyooka et al. showed that epidermal growth factor receptor mutation, but not sex or smoking, is independently associated with a favorable prognosis of gefitinib-treated patients with lung adenocarcinoma [5]. EGFR-TKI treatment should be considered in patients with an EGFR mutation, even if they have a history of smoking or emphysema without fibrosis.

The presence of EGFR mutations in patients with pulmonary fibrosis was rare in this study. Only one (5.9%) of 17 patients with pulmonary fibrosis had an EGFR mutation. Preexisting chronic ILD is known as a risk factor for ILD in gefitinib treatment [10]. In this study, one patient with

Table 3: Characteristics of patients with an EGFR mutation treated with gefitinib.

Total number	43
Age (median, range)	67, 28–92
Gender	
Male	13
Female	30
Smoking-status	
Never	24
Ex/Current	19
Pack-years of smokers (median, range)	33, 2.5–225
Histology	
Adenocarcinoma	42
Squamous cell carcinoma	1
Clinical stage of NSCLC	
IB	2
IIIA	1
IIIB	7
IV	22
Recurrence	11
History of chemotherapy before gefitinib treatment	
No	28
Yes	15
EGFR mutation	
Ex18 G719C	1
Ex19 del	30
Ex21 L858R	10
Ex19 del + Ex21L858R	1
Ex19 del + Ex20 T790M	1
Chest CT	
Normal	36
Emphysema	6
Fibrosis	1

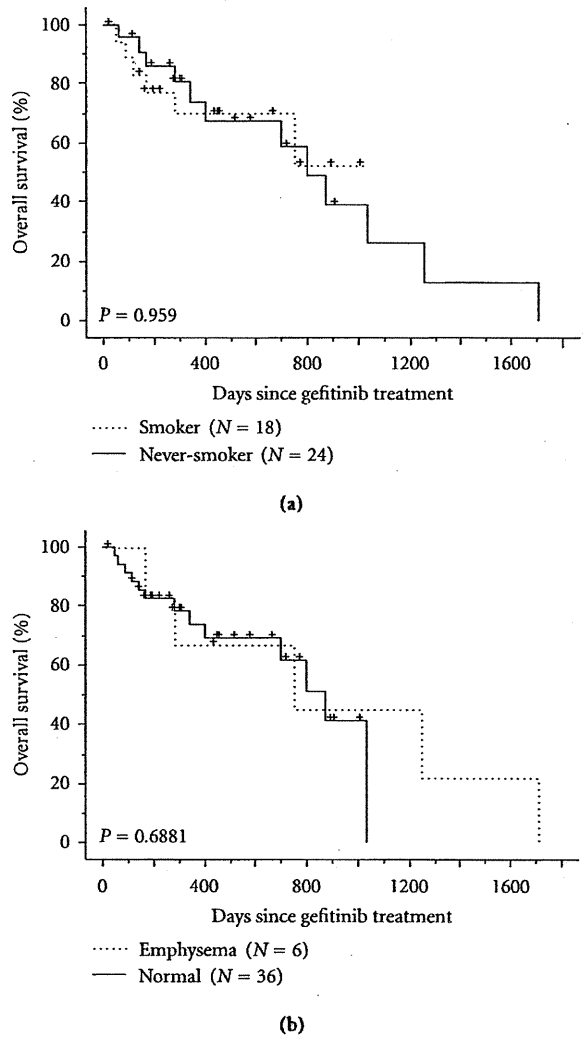

Figure 1: (a) Overall survival of patients with an EGFR mutation treated with gefitinib, according to smoking status (never smokers: solid line; smokers: dotted line). +: censored patient. (b) Overall survival of patients with an EGFR mutation treated with gefitinib, according to underlying pulmonary disease (normal: solid line; emphysema: dotted line). +: censored patient.

pulmonary fibrosis and an EGFR mutation treated with gefitinib developed fatal ILD.

The present study had several limitations, including the fact that it was observational and uncontrolled in design and was performed at a single institution, with retrospective collection of data. The results may have been subject to some selection and treatment bias. The indications for therapy and the selection of treatment were not uniform for all patients, thereby limiting the evaluation of the effects of treatment. The data presented herein should not be interpreted as providing an appropriate evaluation of the efficacy of treatment, which will require randomized prospective studies. A multivariate analysis could not be performed due to the small sample size, and it was therefore not possible to evaluate the potential confounding effects of various other variables related to survival. However, the existence of emphysema and fibrosis on chest CT were prospectively identified at the diagnosis of lung cancer. The EGFR mutation status was identified before the EGFR-TKI treatment. Data on the demographic characteristics and survival of patients were unlikely to be affected by the study design.

In summary, the frequency of EGFR mutations in patients with normal lungs on chest CT was not different between smokers and never-smokers. Of patients with sensitive EGFR mutations and normal lungs on chest CT, smokers had a comparable prognosis with never-smokers. Selecting patients on the basis of chest CT, rather than the smoking status, would likely result in a population with a greater sensitivity to gefitinib.

Conflict of Interests

The authors declare that there is no conflict of interests.

References

[1] M. Fukuoka, S. Yano, G. Giaccone et al., "Multi-institutional randomized phase II trial of gefitinib for previously treated patients with advanced non-small-cell lung cancer," *Journal of Clinical Oncology*, vol. 21, no. 12, pp. 2237–2246, 2003, Erratum in: *Journal of Clinical Oncology*, vol. 22, no. 23, pp. 4811, 2004.

[2] T. J. Lynch, D. W. Bell, R. Sordella et al., "Activating mutations in the epidermal growth factor receptor underlying responsiveness of non-small-cell lung cancer to gefitinib," *New England Journal of Medicine*, vol. 350, no. 21, pp. 2129–2139, 2004.

[3] J. G. Paez, P. A. Jänne, J. C. Lee et al., "EGFR mutations in lung, cancer: correlation with clinical response to gefitinib therapy," *Science*, vol. 304, no. 5676, pp. 1497–1500, 2004.

[4] T. Mitsudomi, T. Kosaka, H. Endoh et al., "Mutations of the epidermal growth factor receptor gene predict prolonged survival after gefitinib treatment in patients with non-small-cell lung cancer with postoperative recurrence," *Journal of Clinical Oncology*, vol. 23, no. 11, pp. 2513–2520, 2005.

[5] S. Toyooka, T. Takano, T. Kosaka et al., "Epidermal growth factor receptor mutation, but not sex and smoking, is independently associated with favorable prognosis of gefitinib-treated patients with lung adenocarcinoma," *Cancer Science*, vol. 99, no. 2, pp. 303–308, 2008.

[6] T. Mitsudomi, S. Morita, Y. Yatabe et al., "Gefitinib versus cisplatin plus docetaxel in patients with non-small-cell lung cancer harbouring mutations of the epidermal growth factor receptor (WJTOG3405): an open label, randomised phase 3 trial," *The Lancet Oncology*, vol. 11, no. 2, pp. 121–128, 2010.

[7] M. Maemondo, A. Inoue, K. Kobayashi et al., "Gefitinib or chemotherapy for non-small-cell lung cancer with mutated EGFR," *New England Journal of Medicine*, vol. 362, no. 25, pp. 2380–2388, 2010.

[8] M. H. Cohen, G. A. Williams, R. Sridhara, G. Chen, and R. Pazdur, "FDA drug approval summary: gefitinib (ZD1839) (Iressa®) tablets," *Oncologist*, vol. 8, no. 4, pp. 303–306, 2003.

[9] M. Ando, I. Okamoto, N. Yamamoto et al., "Predictive factors for interstitial lung disease, antitumor response, and survival in non-small-cell lung cancer patients treated with gefitinib," *Journal of Clinical Oncology*, vol. 24, no. 16, pp. 2549–2556, 2006.

[10] S. Kudoh, H. Kato, Y. Nishiwaki et al., "Interstitial lung disease in Japanese patients with lung cancer: a cohort and nested case-control study," *American Journal of Respiratory and Critical Care Medicine*, vol. 177, no. 12, pp. 1348–1357, 2008.

[11] V. Cottin, H. Nunes, P. Y. Brillet et al., "Combined pulmonary fibrosis and emphysema: a distinct underrecognised entity," *European Respiratory Journal*, vol. 26, no. 4, pp. 586–593, 2005.

[12] K. Usui, C. Tanai, Y. Tanaka, H. Noda, and T. Ishihara, "The prevalence of pulmonary fibrosis combined with emphysema in patients with lung cancer," *Respirology*, vol. 16, no. 2, pp. 326–331, 2011.

[13] A. Sutani, Y. Nagai, K. Udagawa et al., "Gefitinib for non-small-cell lung cancer patients with epidermal growth factor receptor gene mutations screened by peptide nucleic acid-locked nucleic acid PCR clamp," *British Journal of Cancer*, vol. 95, no. 11, pp. 1483–1489, 2006.

[14] R. J. Hung, J. D. McKay, V. Gaborieau et al., "A susceptibility locus for lung cancer maps to nicotinic acetylcholine receptor subunit genes on 15q25," *Nature*, vol. 452, no. 7187, pp. 633–637, 2008.

[15] T. E. Thorgeirsson, F. Geller, P. Sulem et al., "A variant associated with nicotine dependence, lung cancer and peripheral arterial disease," *Nature*, vol. 452, no. 7187, pp. 638–642, 2008.

[16] D. Lambrechts, I. Buysschaert, P. Zanen et al., "The 15q24/25 susceptibility variant for lung cancer and chronic obstructive pulmonary disease is associated with emphysema," *American Journal of Respiratory and Critical Care Medicine*, vol. 181, no. 5, pp. 486–493, 2010.

[17] R. P. Young, R. J. Hopkins, T. Christmas, P. N. Black, P. Metcalf, and G. D. Gamble, "COPD prevalence is increased in lung cancer, independent of age, sex and smoking history," *European Respiratory Journal*, vol. 34, no. 2, pp. 380–386, 2008.

[18] R. Hubbard, A. Venn, S. Lewis, and J. Britton, "Lung cancer and cryptogenic fibrosing alveolitis: a population-based cohort study," *American Journal of Respiratory and Critical Care Medicine*, vol. 161, no. 1, pp. 5–8, 2000.

Lung Cancer 72 (2011) 229–237

Contents lists available at ScienceDirect

Lung Cancer

journal homepage: www.elsevier.com/locate/lungcan

Minichromosome maintenance (MCM) protein 4 as a marker for proliferation and its clinical and clinicopathological significance in non-small cell lung cancer

Junko Kikuchi[a], Ichiro Kinoshita[b,*], Yasushi Shimizu[b], Eiki Kikuchi[a], Kayoko Takeda[b], Hiroyuki Aburatani[e], Satoshi Oizumi[a], Jun Konishi[a], Kichizo Kaga[c], Yoshihiro Matsuno[d], Michael J. Birrer[f], Masaharu Nishimura[a], Hirotoshi Dosaka-Akita[b]

[a] First Department of Medicine, Hokkaido University School of Medicine, North 15, West 7, Kita-ku, Sapporo 060-8638, Japan
[b] Department of Medical Oncology, Hokkaido University Graduate School of Medicine, North 15, West 7, Kita-ku, Sapporo 060-8638, Japan
[c] Department of Surgical Oncology, Hokkaido University Graduate School of Medicine, North 15, West 7, Kita-ku, Sapporo 060-8638, Japan
[d] Department of Surgical Pathology, Hokkaido University Hospital, North 14, West 5, Kita-ku, Sapporo 060-8648, Japan
[e] Genome Science Division, Research Center for Advanced Science and Technology, University of Tokyo, Tokyo 153-8904, Japan
[f] Department of Obstetrics, Gynecology, and Reproductive Biology, Division of Gynecologic Oncology, Brigham and Women's Hospital, Harvard Medical School, Boston, MA 02115, USA

ARTICLE INFO

Article history:
Received 1 April 2010
Received in revised form 7 July 2010
Accepted 19 August 2010

Keywords:
Minichromosome maintenance protein 4
Non-small cell lung cancer
Immunohistochemistry
Proliferation
AP-1
TAM67

ABSTRACT

Background: Minichromosome maintenance (MCM) proteins 2–7 form a complex essential for the initiation of DNA replication. In the process to screen expression changes related to growth suppression of non-small cell lung cancer (NSCLC) cells by a cJun dominant-negative mutant, we found that reduced expression of MCM4 was correlated with this growth suppression.
Method: We determined the relevance of MCM4 in proliferation of NSCLC by downregulating its expression with small-interfering RNA in three NSCLC cell lines. We then immunohistochemically analyzed MCM4 expression in 156 surgically resected NSCLCs to correlate clinicopathologic characteristics.
Results: MCM4 downregulation reduced proliferation in two cell lines. MCM4 expression was higher in cancer cells than in adjacent normal bronchial epithelial cells ($p < 0.001$). High MCM4 expression was correlated with male gender, heavy smoking, poorer differentiation and non-adenocarcinoma histology ($p < 0.001$, respectively). High MCM4 expression was also correlated with proliferation markers, Ki-67 and cyclin E expression ($p < 0.001$, respectively). MCM4 expression was not associated with survival.
Conclusion: MCM4 may play an essential role in the proliferation of some NSCLC cells. Taken together with higher expression in NSCLCs and its correlation with clinicopathologic characteristics such as non-adenocarcinoma histology, MCM4 may have potential as a therapeutic target in certain population with NSCLCs.

1. Introduction

Lung cancer is a leading cause of cancer death worldwide, and non-small cell lung cancer (NSCLC) accounts for more than 80% of all lung cancer cases. Despite some advances in early detection and recent improvements in treatment, prognosis of patients with lung cancer remains poor [1,2]. The current challenge is to identify new therapeutic targets and strategies, and to incorporate them into existing treatment regimens with the goal of improving therapeutic gain.

We have previously shown that blocking AP-1 transcription factor by a cJun dominant-negative mutant, TAM67, inhibited growth of non-small cell lung cancer (NSCLC) cells including NCI-H1299 (H1299) cells [3,4]. To identify effectors relevant to the growth inhibition, we performed microarray analysis and found that TAM67 decreased mRNA levels of minichromosome maintenance (MCM) protein 4 in H1299 cells.

MCM4 is one of six MCM proteins composing the prereplicative complex that binds to replication origins in the G1 phase of the cell cycle and is essential for the initiation of DNA replication [5–7]. After initiation of replication, MCM proteins dissociate from the origin, and this prevents a second round of DNA replication from the same origin during the same S phase. These proteins are also required for unwinding parental DNA strands during replication fork progression [8].

It has recently been reported that MCM immunoreactivity is a specific and accurate marker for proliferating cells [9,10]. Some of these studies have indicated the superior sensitivity of MCM proteins over the standard proliferation marker Ki67, which resides in the fact that these biomarkers identify not only cycling cells but

* Corresponding author. Tel.: +81 11 706 5551; fax: +81 11 706 5077.
E-mail address: kinoshii@med.hokudai.ac.jp (I. Kinoshita).

0169-5002/$ – see front matter © 2010 Elsevier Ireland Ltd. All rights reserved.
doi:10.1016/j.lungcan.2010.08.020

also non-cycling cells with proliferative potential [10]. In addition, several groups have demonstrated that dysregulation of MCM proteins is an early event in tumorigenesis and have exploited these biomarkers in primary diagnosis, tumor surveillance and prognosis in a range of tumor types [11–14].

Although several studies have assessed MCM2 in lung cancer [15–18], there have been no reports determining relevance of MCM4 in proliferation of NSCLC cells or evaluating the expression of MCM4 in NSCLC tissues. Therefore, we analyzed the effects of MCM4 downregulation by small-interfering RNA (siRNA) in NSCLC cell lines and MCM4 expression by Immunohistochemistry in a cohort of 156 surgically resected NSCLCs in order to correlate clinicopathological characteristics.

2. Material and methods

2.1. Cell lines and culture conditions

The human NSCLC cell lines NCI-H1299 (H1299), A549, NCI-H520 (H520), LK-2, NCI-H209 (H209), (American Type Culture Collection, Manassas, VA, USA), PC-3, LK-2 (Japan Cancer Research Resources Bank, Tokyo, Japan) were cultured in RPMI 1640 medium (Invitrogen Life Technologies, Inc., Carlsbad, CA, USA) supplemented with 10% fetal bovine serum (FBS) and 0.03% glutamine at 37 °C in an atmosphere of 5% CO_2. H1299 cells expressing TAM67 in a doxycycline-controlled manner (H1299-TAM67 Tet-on clone cells) were established from parental H1299 cells as described previously [3]. BEAS2B (American Type Culture Collection) was cultured in LHC-9 medium (Invitrogen).

2.2. siRNA transfection

RNA interference of MCM4 was performed using 21-bp (including a 2-deoxynucleotide overhang) siRNA duplexes purchased from Ambion (Ambion Inc. Austin, TX, USA). The target sequence for hMCM4 was GGCUCUCAUCGAGGCUUAUtt. A negative control siRNA was provided by an irrelevant, “unrelated” siRNA comprising a 19 bp scrambled sequence. Transfection was carried out using 11 nM siRNA oligonucleotide duplexes with Lipofectamine 2000 (Invitrogen) according to the manufacturer's recommendations.

2.3. Microarray analysis and quantitative real-time reverse transcription-PCR

Total RNA was isolated using TRIzol (Invitrogen) from H1299 Tet-on clone cells grown in the absence or presence of doxycycline (2 μg/ml). RNAs were analyzed on GeneChip HG U133 oligonucleotide arrays (Affymetrix, Santa Clara, CA, USA) containing probes for 40,000 human genes. Microarray analysis was essentially performed as described previously [19]. Further information on the source of other RNAs from normal tissues analyzed here is available at http://www.lsbm.org/database/index.html. A total of 77 genes had a two-fold fewer or greater signal in the H1299 cells with TAM67 induction relative to those without induction of TAM67 (using baseline analysis by Microarray Suite 5.0t).

Quantitative real-time reverse transcription-PCR (RT-PCR) was performed on a TaqMan ABI 7000 Sequence Detection System (Applied Biosystems, Foster City, CA, USA). The gene-specific primers and TaqMan probes used are available as TaqMan Gene Expression Assays (Applied Biosystems) for MCM4 (Hs00381533_m1) and GAPDH (4326317E). An identical set of PCR cycle parameters was used for all genes: 50 °C for 2 min, 95 °C for 10 min and 40 cycles of 95 °C for 15 s and 60 °C for 1 min, as validated by Applied Biosystems. GAPDH mRNA was used as an endogenous control for quantification. Quantitative analysis of cDNA was performed based on the comparative Ct technique.

2.4. Cell growth assays

Cells were seeded at 800–1500 cells/well in 96-well plates in normal growth medium. Transfection was performed at a confluence of 30–50% with 11 nM siRNA and Lipofectamine 2000 reagent every 72 h. After 7 days, anchorage-dependent growth was measured in 96-well plates using an MTT (dimethyl thiozolyl-2′, 5′-diphenyl-2-*H*-tetrazolium bromide)-based assay (non-radioactive proliferation assay, Promega Corp., Madison, WI, USA).

2.5. Western blot analysis

Western blot analysis was essentially performed as described previously [3]. Equal amounts of protein were separated on 12 or 15% SDS gels, transferred to nitrocellulose membranes (Amersham Biosciences, Inc. St. Albans, UK), and incubated with anti-MCM4 antibody (sc-28317, Santa Cruz Biotechnology, Santa Cruz, CA, USA). Primary antibody was detected using anti-mouse antibody conjugated with horseradish peroxidase (NA931V, Amersham Biosciences Inc.) and visualized using the Amersham ECL system. Band intensity after Western blotting was determined by laser scanning of the films followed by quantitative densitometric analysis using NIH Image Ver 1.62 software. Standardization was performed with actin measured in the same blots with anti-actin antibody (A-2066, Sigma-Aldrich Co., St. Louis, MO, USA).

2.5.1. Cell cycle analysis

Cells were cultured in 100-mm plates. Transfection was performed at a confluence of 30–50% with 11 nM siRNA. After 3 days, cells were trypsinized, washed twice with PBS, and fixed in 70% ethanol at −20 °C. Fixed cells were centrifuged and resuspended in 250 μg/ml RNase and 50 μg/ml propidium iodide (PI) (Sigma) for DNA staining. DNA content was measured by a FACScan flow cytometer (Becton Dickinson, San Jose, CA, USA) and two software packages: CellQuest 3.1 (BD Pharmingen, San Diego, CA, USA) and ModFit LT 2.0 (Verity Software House, Topsham, ME, USA).

2.5.2. Apoptosis analysis

Cells were stained with FITC-conjugated annexin V and PI, using Annexin V-FITC Apoptosis Detection kit (Calbiochem Inc., Darmstadt, Germany). Briefly, cells were trypsinized, centrifuged at 1000 g for 5 min, washed one time with ice-cold PBS and resuspended in 500 μl of binding buffer. Thereafter, 1.1 μl of Annexin V-FITC and 10 μl of PI were added and mixed for 15 min in the dark. The percentage of apoptotic cells was measured by a FACScan flow cytometer (Becton Dickinson). Data analysis was performed using CellQuest 3.1 (BD Pharmingen).

2.6. Tumor specimens and survival data

The present study included 156 patients (105 men and 51 women) for whom adequate archival primary tumor specimens were consecutively obtained by radical surgical treatment at Hokkaido University Medical Hospital between 1982 and 1994. Histological diagnosis and grade of differentiation were determined in accordance with World Health Organization criteria [20]. Specimens included 65 squamous cell carcinomas, 82 adenocarcinomas, 2 large cell carcinomas, and 7 adenosquamous cell carcinomas. For this study, non-adenocarcinoma included squamous cell carcinoma, large cell carcinoma, and adenosquamous cell carcinoma. Pathological stage (pStage) was based on the American Joint Committee on Cancer guidelines for postoperative tumor-node-metastasis (TNM) [21]. The specimens represented tumors of

pStage I ($n=90$), pStage II ($n=24$), pStage III ($n=38$), and pStage IV ($n=4$). Survival was analyzed for the 145 patients who met the following criteria: (a) survived for more than 3 months after surgery; (b) did not die of causes other than lung cancer within 5 years after surgery; and (c) were followed for more than 3 years after surgery (for patients who remained alive). Survival data were updated in May 2006, and the median follow-up time among patients who did not die was 3349 days (range, 1184–5830). Samples from normal liver, cardiac muscle, adrenal gland and normal colon were obtained from autopsy cases died of other disease. In all cases, informed consent was obtained for the use of resected specimens. This study was approved by the Medical Ethics Committee of Hokkaido University Hospital.

2.7. Immunohistochemical analysis

MCM4 expression was analyzed by immunohistochemistry as described previously [22]. The labeled streptavidin biotin method was used on 4-μm sections of formalin-fixed, paraffin-embedded tissues after deparaffinization. Briefly, deparaffinized tissue sections were treated with an autoclave in 10 mM citrate buffer (pH 6.0) for 20 min at 121 °C in order to retrieve antigenicity. Sections were then immersed in methanol containing 1.5% hydrogen peroxide for 20 min to block endogenous peroxidase activity, and were further incubated with normal rabbit serum to block nonspecific antibody binding sites. Sections were reacted consecutively with mouse monoclonal anti-MCM4 antibody (Santa Cruz Biotechnology), at a dilution of 1:50 at 4 °C overnight. Immunostaining was performed by the biotin-streptavidin immunoperoxidase method with 3,3-diaminobenzidine as a chromogen (SAB-PO kit; Nichirei, Tokyo, Japan). Hematoxylin solution was used for counterstaining. Blocks of H1299 cells treated with or without MCM4 siRNA acted as positive or negative controls. Tumor cells were considered MCM4 positive if any nuclear staining was present.

MCM4 labeling index (LI) in tumor cells (%) was defined as the percentage of tumor cells displaying nuclear immunoreactivity and was calculated by counting the number of MCM4-nuclear stained tumor cells in 500 tumor cells in each section. A single representative tissue section from each tumor was surveyed microscopically at ×100 for at least two or three areas with highest MCM4 intensity of positive tumor cells. MCM4 LI in the adjacent normal bronchial epithelial cells (%) was defined as the percentage of bronchial epithelial cells displaying nuclear immunoreactivity and was calculated by counting the number of MCM4-nuclear stained bronchial epithelial cells in up to a maximum of 500 bronchial epithelial cells for areas with highest MCM4 intensity in each section.

Immunohistochemical evaluations were assessed twice using a BX 40 microscope (Olympus, Tokyo, Japan) by one investigator (J.K.) who was blinded to the status of other immunohistologic and clinical data, and were reproducibly obtained.

2.8. Statistical analysis

Statistical inferences in comparative experiments in vitro were obtained using unpaired, two-sided Student's *t*-test. Associations between MCM4 expression and categorical variables were analyzed by χ^2 test or Fisher's exact test, as appropriate. To simultaneously examine the effects of more than one factor on MCM4 expression, multivariate logistic regression analysis was used. Interrelationships between MCM4 and Ki-67 were analyzed by Pearson's correlation coefficient. LIs for MCM4 and Ki-67 were compared by non-parametric Mann–Whitney *U*-test. LIs for MCM4 in cancer cells were compared to those in adjacent normal bronchial epithelial cells using Wilcoxon matched pairs signed ranks test. Survival curves were estimated using the Kaplan–Meier method, and differences in survival distributions were evaluated by log-rank test.

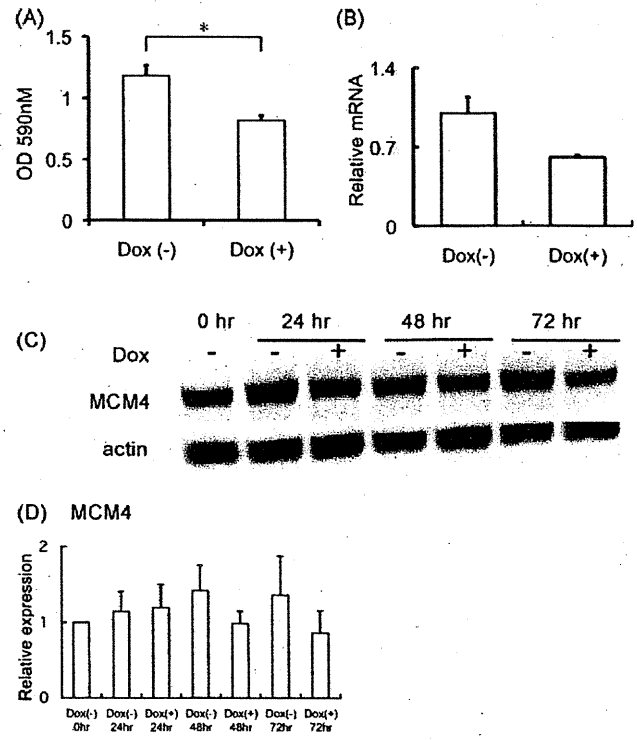

Fig. 1. (A) Growth inhibition by induction of TAM67. H1299 Tet-on TAM67 clone cells were cultured in the absence or presence of doxycycline for 3 days. Cell growth was measured by 3-(4,5-dimethylthiazol-2-yl)-2,5-diphenyltetrazolium bromide (MTT) assay. Values represent the means ± S.D. ($n=4$). *$p<0.01$. (B) Quantitative real-time PCR of MCM4 mRNA. H1299 Tet-on TAM67 clone cells were cultured in the absence or presence of doxycycline for 24 h. Standardization was with GAPDH mRNA. MCM4 mRNA levels in the presence of doxycycline were compared to those in the absence of doxycycline at 24 h (set equal to 1). (C and D) Western blot analysis of MCM4. H1299 Tet-on TAM67 clone cells were cultured in the absence or presence of doxycycline for 72 h. Standardization was against actin measured in the same blots. Protein expression levels among the various conditions were compared based on the ratio of expression of a protein under each condition to that in the absence of doxycycline at 0 h (set as 1). Data show the mean value of three independent experiments with error bars representing S.D. NIH image 1.62 software was used to densitize and quantify the bands.

The level of significance was set at $p<0.05$. Statistical analyses were performed using SPSS version 11.0.

3. Result

3.1. Induction of a cJun dominant-negative mutant, TAM67 decreased MCM4

We previously isolated H1299 clones that express TAM67 under the control of an inducible promoter, the tet-on promoter, and showed that induction of TAM67 inhibits growth of H1299 Tet-on clone cells (Fig. 1A, [3,4]). To identify downstream effectors relevant to the growth inhibition, we performed microarray analysis. MCM4 expression decreased two-fold with induction of TAM67, and we focused on it because of its role as a regulator of the cell cycle. To confirm the array data, we performed real-time quantitative PCR and Western blot analysis. We confirmed that expression of MCM4 mRNA and protein decreased by 40–50% and 20–30%, respectively, when TAM67 was induced (Fig. 1B–D).

3.2. Inhibition of MCM4 expression by siRNA reduced cell proliferation in NSCLC cell lines

Next, we investigated whether this gene is relevant to cell proliferation using siRNA to reduce the levels of MCM4 protein in three

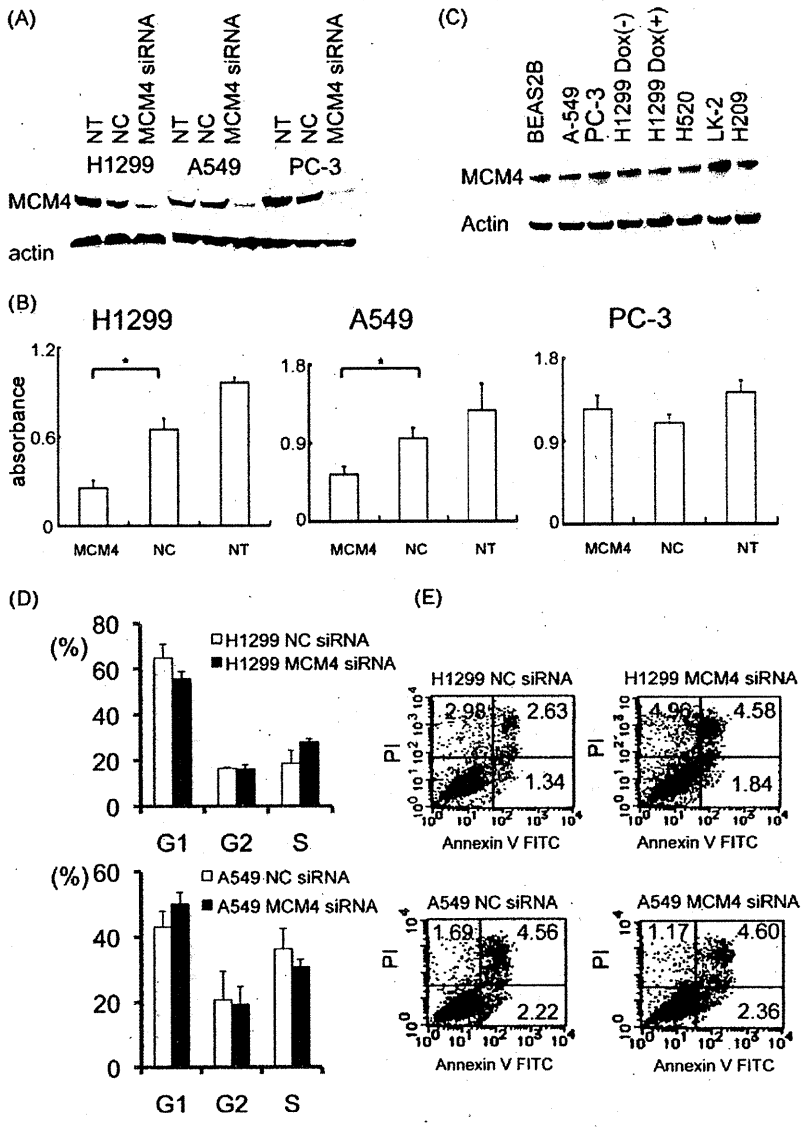

Fig. 2. (A) Western blot analysis of MCM4 in H1299, A549 and PC-3. Cell lysates were collected at 3 days after transfection with MCM4 or negative control siRNA and were subjected to Western blot analysis. NT; non-transfectant, NC; transfected with negative control siRNA. (B) Effects of MCM4 knockdown on cell growth in three lung cancer cell lines. H1299, A549 and PC-3 were transfected with MCM4 or negative control siRNA every 72 h. After 7 days, cell growth was measured using MTT assay. Data points are means ± S.D. of quadruplet samples in one of the three independent experiments. $^{*}p < 0.01$ versus cells treated with negative control siRNA. (C) Western blot analysis of MCM4 in NSCLC cell lines, a SCLC cell line (NCI-H209) and an immortalized bronchial epithelial cell line (BEAS2B). (D) Effect of MCM4 knockdown on cell cycle in H1299 and A549. Cells were transfected with MCM4 or negative control siRNA. After 72 h, the percentage of cells in each phase was measured by a FACS flow cytometer and analyzed using ModFitLT software. The data show the average percentage of three independent experiments with error bars representing the S.D. (E) Cell apoptosis analysis of H1299 and A549 cells by flow cytometry using staining of Annexin V-FITC and PI. Cells were transfected with MCM4 or negative control siRNA. After 72 h, the percentage of cells of apoptotic fraction was measured by a FACS flow cytometer. Representative data of three independent experiments. The cells that took up PI but did not bind Annexin V-FITC would most likely be necrotic were shown in the upper left quadrant; late apoptotic cells that bind Annexin V-FITC and PI in upper right quadrant; early apoptotic cells binding Annexin V-FITC in lower right quadrant; viable cells binding neither Annexin V-FITC nor PI in lower left quadrant.

NSCLC cell lines; H1299, A549 and PC-3. Reduction of MCM4 protein expression in these three NSCLC cell lines was confirmed by Western blot analysis (Fig. 2A). H1299 and A549 cells transfected with MCM4 siRNA exhibited decreased cell growth when compared to cells transfected with negative control siRNA, while the reduction in MCM4 protein did not inhibit cell growth of PC-3 cells (Fig. 2B).

MCM4 expression levels of NSCLC cell lines, a SCLC cell line (NCI-H209) and an immortalized bronchial epithelial cell line, BEAS2B were various but not very different (Fig. 2C).

We used flow cytometry to determine if growth inhibition was due to cell cycle arrest or apoptosis in H1299 and A549 cells (Fig. 2D and E). Cell cycle analysis revealed that H1299 cells transfected with MCM4 siRNA exhibited S phase arrest when compared to cells transfected with negative control siRNA, while A549 cells transfected with MCM4 siRNA exhibited G1 cell cycle arrest compared to those transfected with negative control siRNA (Fig. 2D). Sub-G1 fraction was observed in H1299 cells transfected with MCM4 siRNA (data not shown). Flow cytometry analysis using Annexin V and propidium iodide demonstrated that H1299 cells transfected with MCM4 siRNA exhibited increase in apoptotic fraction compared to those transfected with negative control siRNA, while the transfection of MCM4 siRNA did not increase apoptotic fraction in A549 cells (Fig. 2E).

3.3. *Immunohistochemical analysis*

Typical immunohistochemistry patterns for MCM4 in NSCLCs are shown in Fig. 3A. H1299 cells showed diffuse and abundant

MCM4-nuclear expression, while those treated with MCM4 siRNA showed negative expression, except for sporadic expression in few cells. These cell blocks were included as positive or negative external control with each batch of staining. MCM4 expression was consistently found in the nuclei of tumor cells. As MCM4 positive cells were observed more in the marginal area of the tumor than in the center, as reported previously [18], we primarily evaluated the marginal areas. Normal bronchial epithelial cells and alveolar pneumocytes adjacent to tumors showed various nuclear MCM4 expression patterns, consistent with previous findings that MCM2 and MCM5 are seen in less than 25% of normal bronchial epithelial cells and less than 15% of alveolar pneumocytes [9].

Fig. 3B and C shows a histogram for the distribution of MCM4 LIs in tumors (Fig. 3B) and adjacent normal bronchial epithelial cells (Fig. 3C). MCM4 LIs were significantly higher in cancer cells than in the adjacent normal bronchial epithelial cells (median LIs 76.1 vs. 64.7%; $p < 0.001$ by Wilcoxon matched pairs signed ranks test).

Tissue-wide expression profiles of the MCM4 gene showed that expression in lung cancer tissues and lung cancer cell lines were higher than in various normal tissues, including lung and trachea, except for testis and bone marrow (Fig. 3D). Immunohisotochemical analysis of samples from normal liver, cardiac muscle and adrenal gland showed negative expression and a sample from normal colon showed only sporadic expression in colon

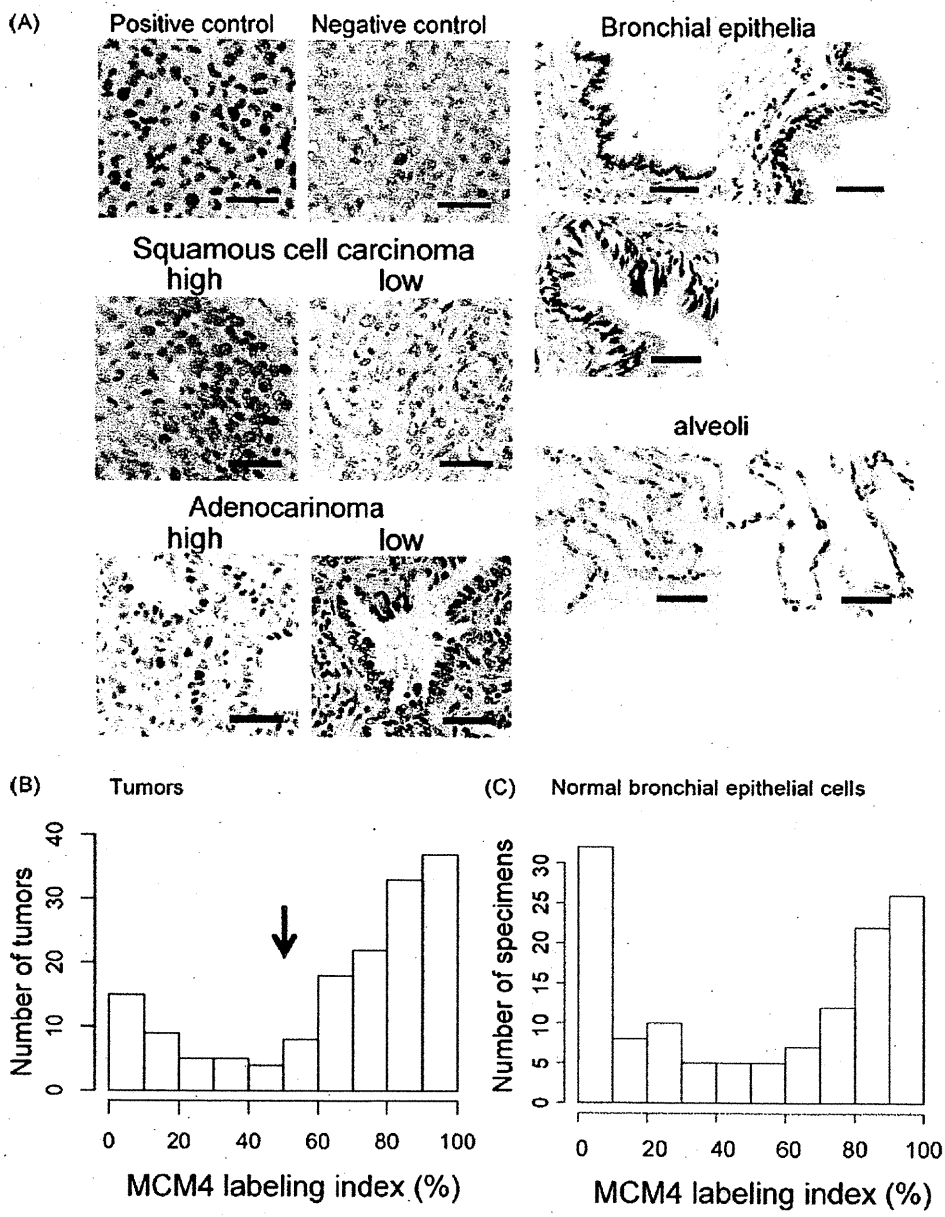

Fig. 3. (A) Immunohistochemical staining patterns for MCM4 in NSCLCs. NSCLC specimens were stained with anti-MCM4 antibody. MCM4 expressions in normal bronchial and alveolar cells are also shown (Scale bar = 50 μm). H1299 cells treated with or without MCM4 siRNA served as positive or negative controls. (B) Distribution of MCM4 expression in NSCLCs. A histogram for the distribution of nuclear MCM4 expression of any intensity in 156 NSCLCs is shown. Mean ± S.D. and median labeling indices of tumors were 65.8 ± 30.1 and 76.1%, respectively. Arrow, proposed cutoff level for MCM4 labeling index (50%) for the present study. (C) Distribution of MCM4 expression in normal bronchial epithelial cells adjacent to tumors. A histogram for the distribution of nuclear MCM4 expression of any intensity is shown in 132 NSCLC specimens, in which bronchial epithelial cell was evaluated. Mean ± S.D. and median labeling indices of bronchial epithelial cells were 52.5 ± 36.4 and 64.7%, respectively. MCM4 expression was significantly higher in cancer cells than in the adjacent normal bronchial epithelial cells ($p < 0.001$). (D) Tissue-wide expression of MCM4. Signal denotes gene expression level obtained from microarray analysis. (a) 26 normal tissues, (b) 5 fetal tissues, (c) 6 cultured normal cells, (d) 21 lung cancers and (e) 8 lung cancer cell lines. (E) Immunohisotochemical analysis of a sample from normal colon, liver, cardiac muscle and adrenal gland.

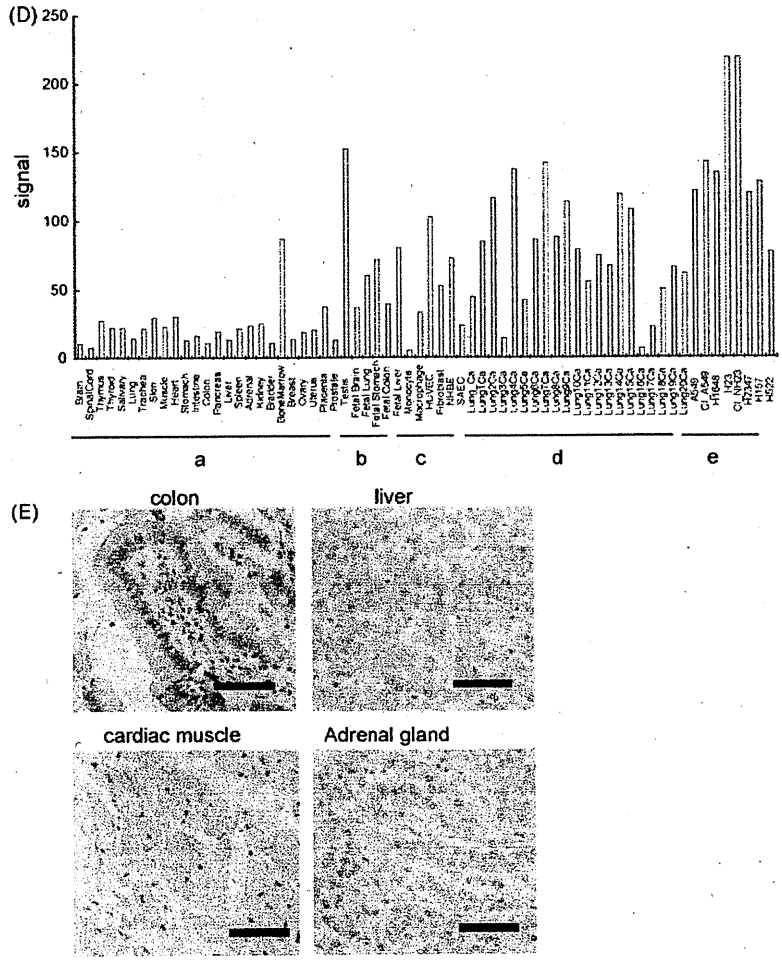

Fig. 3. (*Continued*).

epithelial cells, consistent with the tissue-wide expression profiles (Fig. 3E).

The MCM4 LIs for tumor cells showed a marked downward convex trend and consisted of two populations with a cutoff level of 50%. The tumors were accordingly divided into a group with MCM4 LIs < 50%, and another group with MCM4 LIs ≥ 50%, subsequently referred to as “low” and “high” MCM4 expression, respectively. High MCM4 expression was found in 118 (75.6%) NSCLCs. χ^2 test or Fisher's exact test revealed that high MCM4 expression was significantly correlated with tumors from men ($p < 0.001$), smoking history ($p < 0.001$), non-adenocarcinoma histology ($p < 0.001$), poorer differentiation ($p < 0.001$) and advanced pT classification ($p = 0.05$) (Table 1). Multivariate logistic regression analysis of the correlation between MCM4 expression and various characteristics showed a significant association between high MCM4 expression and non-adenocarcinoma (adjusted odds ratio; 7.04, $p = 0.004$; Table 2).

Among biological characteristics of tumors studied previously in this cohort of NSCLCs [22,23], Ki-67 and cyclin E expression was correlated with high MCM4 expression ($p < 0.001$, respectively, Table 3). As expected, MCM4 LIs were significantly higher than the Ki-67 LIs ($p < 0.001$, Fig. 4A). The two markers showed a significant correlation ($r = 0.39$, $p < 0.001$, Fig. 4B), which was also expected.

We next analyzed the relationship between MCM4 expression and patient survival (Fig. 5). Patients having tumors with high or low MCM4 expression did not display apparent difference in survival ($p = 0.5$).

4. Discussion

The present study demonstrated the growth suppressive effects of MCM4 downregulation in certain NSCLC cell lines and the deregulated expression of MCM4 in cancer tissues, as well as its correlation with clinicopathological characteristics such as non-adenocarcinoma histology and proliferation markers, Ki67 and cyclin E. Although previous studies have assessed MCM2 in lung cancer [15–18], there have been no reports determining relevance of MCM4 in proliferation in NSCLC cells, or evaluating expression of MCM4 in NSCLC tissues and its clinicopathological significance.

Growth suppression induced by MCM4 knockdown in H1299 and A549 cells is expected based on its essential role in DNA replication. Intriguingly, MCM4 knockdown induced S phase arrest and slight apoptosis in H1299, while it induced G1 arrest in A549. Gradual depletion of maternally derived MCM5 protein leads to a prolonged S phase, cell-cycle-exit failure, apoptosis, and reduction in cell number in $mcm5^{m850}$ mutant zebrafish embryos [24]. In a mouse genetic model, homozygosity for a disrupted MCM4 allele ($MCM4^{-/-}$) caused preimplantation lethality [25]. For human cells, Shreeram et al. [26] reported that inhibition of replication licensing by geminin, which reduced the quantity of MCM2 bound to chromatin, blocked cell proliferation due to S phase arrest and apoptosis in some cell lines including H1299. In contrast, primary fibroblast over-expressing geminin arrested in G1 phase with no detectable apoptosis [26]. Taken together, multiple mechanisms including G1 arrest and S phase arrest with apoptosis may be involved in growth

Table 1
Relationship between MCM4 expression and clinical and clinicopathogical characteristics in 156 surgically resected NSCLCs.

Characteristics	MCM4 expression		p
	Low	High	
Age (yrs)			
<65	21	54	0.4
≥65	17	64	
Sex			0.001
Male	13	92	
Female	25	26	
Smoking			<0.001
Nonsmoker	19	19	
Smoker	16	87	
Smoking (pack-years)			<0.001
$0 \le x \le 20$	23	25	
≥20	12	81	
Histology			
Adenocarcinoma	34	48	<0.001
Squamous	3	61	
Other	1	9	
Differentiation			
Well	19	24	<0.001
Moderate	16	48	
Poor	0	37	
pT classification			
T1	15	26	0.05
T2–T4	23	92	
pN classification			
NO	22	80	0.3
N1–N3	16	38	
pStage			0.9
1	20	70	
2	7	17	
3	10	28	
4	1	3	

NSCLC: non-small cell lung cancer.
Squamous: squamous cell carcinoma.
Other: large cell carcinoma and adenosquamous cell carcinoma.

Table 2
Multivariate logistic regression analysis for the correlation between MCM4 expression and clinical and clinicopathological characteristics.

Variables[a]	Adjusted odds ratio	p
Gender (male/female)	2.84 (0.25–13.0)	0.2
Smoking (smoker/nonsmoker)	1.73 (0.38–7.80)	0.5
Histology (nonadeno[b]/adenocarcinoma)	7.04 (1.84–27.0)	0.004
Differentiation (moderate and poor/well)	1.10 (0.38–3.17)	0.9
pT (T2-4/T1)	1.80 (0.62–5.17)	0.3

[a] Selected from Table 1.
[b] Including squamous cell carcinoma, large cell carcinoma, and adenosquamous cell carcinoma.

Table 3
Relationship between MCM4 expression and cell biological characteristics.

Characteristics	MCM4 expression		p
	Low	High	
Ki-67			<0.001
High	10	82	
Low	21	33	
$p27^{KIP1}$			0.8
High	25	101	
Low	4	13	
cyclin E			<0.001
High	3	78	
Low	28	38	

Ki-67 high; labeling indices ≥30%.
p27 low; labeling indices ≥5%.
cyclin E high; labeling indices ≥30%.

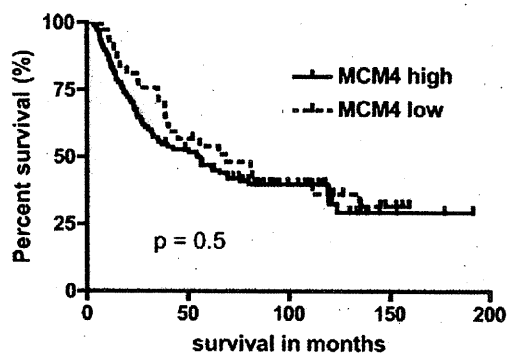

Fig. 5. Kaplan–Meier survival curves of patients with radically resected NSCLCs. Survival curves were stratified by the MCM4 labeling index (LI). MCM4 high; MCM4 LI ≥ 50%. MCM4 low; MCM4 LI < 50%. High and low MCM4 expressions showed no relationship with survival.

suppression by inhibition of the replication licensing system, plausibly dependent on the cell type.

In contrast to H1299 and A549 cells, PC-3 cells did not show growth suppression after MCM4 knockdown in this study. This may be due to differences in the sensitivity of these cell lines to MCM4 inhibition. In the zebrafish genetic model, increased apoptosis is detectable only in the retina, tectum and hindbrain by the third day of development, but not in other late-proliferating tissues, thus suggesting that different tissues may employ distinct cellular programs in responding to the depletion of MCM5 [24]. Different lineages of tumor cells might also show distinct responses to depletion or inhibition of MCM proteins. PC-3 harbors epidermal growth factor receptor (EGFR) mutation [27], although H1299 and A549 do

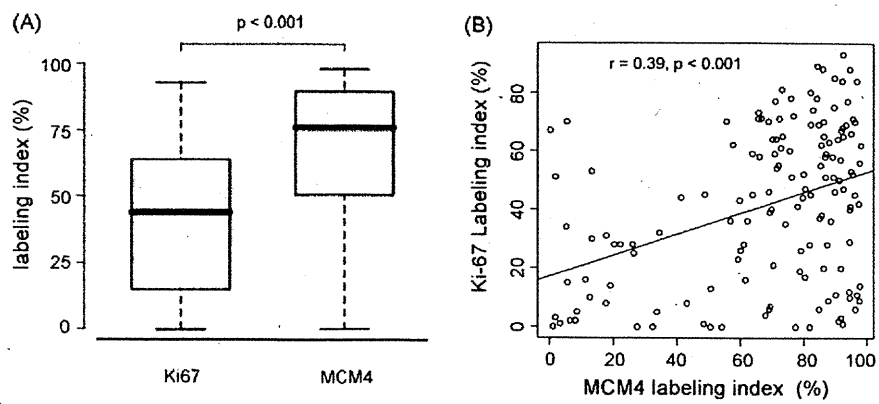

Fig. 4. (A) MCM4 and Ki-67 labeling indices (LIs) in 156 NSCLCs. MCM4 LIs were significantly higher than Ki-67 LIs ($p < 0.001$). Horizontal lines, median; boxes, 25–75% range; brackets, 10–90% range. (B) MCM4 and Ki-67 expression in 156 NSCLCs showed a significant correlation ($r = 0.39$, $p < 0.001$).

not. EGFR mutations are shown to be involved specifically in terminal respiratory unit-type adenocarcinomas, a recently proposed lineage of lung adenocarcinoma with distinct molecular based classification and phenotypic profiles [28,29]. Such hypothesis remains to be tested in future studies.

Given that MCMs play a critical role in the initiation of DNA synthesis and DNA replication, their expression is expected to correlate with cell proliferation. It has been claimed that MCMs represent a potentially more accurate means determining the proliferative fraction within a tumor than conventional proliferation index such as Ki-67, probably because the latter fail to label cells in early G1 [10,30] or are downregulated early in the differentiation program. In contrast, MCMs are downregulated later when the cells adopt a terminally differentiated phenotype [31,32]. Thus, the clinical relevance of MCM proteins as proliferation markers has been determined immunohistochemically in various malignant tumors including NSCLCs [12–15]. These studies focused on the detection of MCM2 or 7, and few investigations have studied MCM4 expression to date [33,34]. The correlation between MCM4 LIs and Ki-67 LIs and the significantly higher MCM4 LIs than Ki-67 LIs in the present study are consistent with the results of MCM2 or 7. This finding suggests that MCM4 may prove to be a more sensitive marker for proliferation in NSCLCs. Although we previously reported that patients with tumors having a high Ki-67 LIs survived for a significantly shorter time than patients with tumors having a low Ki-67 LIs in this cohort [23], the present analysis did not demonstrate MCM4 expression to be a significant prognostic factor. Reflecting considerably higher expression of MCM4 than Ki-67, tumors with high MCM4 and low Ki-67 LIs accounted for almost 60% of tumors with low Ki-67 LIs (Fig. 4B and data not shown). Patients with such high MCM4 and low Ki-67 LIs survived for almost the same period as patients with low MCM4 and Ki-67 LIs who showed favorable prognosis in this cohort (data not shown). We speculate that tumors with high MCM4 and low Ki-67 LIs may contain more cells in early G1 or adopting a terminally differentiated phenotype as discussed above, which might be associated with favorable prognosis, and be a possible reason for the discrepancy between MCM4 and Ki-67 expressions regarding a prognositic role in the present study. Prognostic significance of MCM4 remains to be elucidated in larger cohorts in NSCLCs.

The modestly higher expression of MCM4 in lung cancer tissues, as compared to adjacent bronchial epithelial cells or various normal tissues other than testis and bone marrow, is consistent with previous findings that MCM proteins are strongly expressed in human cancer cells and pre-cancerous cells undergoing malignant transformation [35], and that they are not expressed in differentiated somatic cells that have been withdrawn from the cell cycle [9]. The association between MCM4 expression in tumors and male gender, smoking, non-adenocarcinoma histology, more poorly differentiated tumors and advanced pT classification agree with previous reports showing that high MCM2 or 7 expression is associated with male gender, non-adenocarcinoma histology, more poorly differentiated tumors in NSCLCs [15,17,18,36]. Taken together with the growth suppressive effects by knockdown of this protein in some NSCLC cells, MCM4 may have potential as a therapeutic target in certain populations with NSCLCs, as suggested previously [35].

MCM4 expression did not display an apparent prognostic effects in the present study, which is inconsistent with previous studies on NSCLCs. Ramnath et al. reported that MCM2 is an independent predictor of survival, and others have reported MCM2 combined with Ki-67 or gelsolin is associated with poor prognosis in patients with NSCLCs [15,17,18]. Recently, Fujioka et al. reported that MCM7, but not MCM2, is significantly correlated with poor prognosis in patients with small lung adenocarcinomas [36]. Prognostic significance of MCM4 and other MCM proteins in lung cancer remains to be clarified.

We have previously shown that blocking AP-1 transcription factor by TAM67 inhibited the growth of NSCLC cells [3,4]. We confirmed that the induction of TAM67 decreased expression of MCM4 and inhibition of MCM4 expression by siRNA reduced cell proliferation in H1299 cell, thus suggesting that TAM67 inhibits cell proliferation partially due to reduced expression of MCM4 in H1299 cells. It remains to be determined how TAM67 reduces MCM4 expression.

In conclusion, MCM4 plays an essential role in the proliferation of some NSCLC cells and is a novel proliferative marker in NSCLCs. Taken together with the higher expression in NSCLCs and its correlation with clinicopathological characteristics, such as non-adenocarcinoma histology, MCM4 may have potential as a therapeutic target in certain populations with NSCLCs.

Conflict of interest

There is no conflict of interest.

Acknowledgement

This study was supported in part by a Grant-in-Aid for Scientific Research (C) from the Japan Society for the Promotion of Science.

References

[1] Parkin DM. Global cancer statistics in the year 2000. Lancet Oncol 2001;2:533–43.
[2] Jemal A, Siegel R, Ward E, Hao Y, Xu J, Thun MJ. Cancer statistics, 2009. CA Cancer J Clin 2009;59:225–49.
[3] Shimizu Y, Kinoshita I, Kikuchi J, Yamazaki K, Nishimura M, Birrer MJ, et al. Growth inhibition of non-small cell lung cancer cells by AP-1 blockade using a cJun dominant-negative mutant. Br J Cancer 2008;98:915–22.
[4] Kikuchi J, Kinoshita I, Shimizu Y, Oizumi S, Nishimura M, Birrer MJ, et al. Simultaneous blockade of AP-1 and phosphatidylinositol 3-kinase pathway in non-small cell lung cancer cells. Br J Cancer 2008;99:2013–9.
[5] Romanowski P, Madine MA. Mechanisms restricting DNA replication to once per cell cycle: the role of Cdc6p and ORC. Trends Cell Biol 1997;7:9–10.
[6] Tye BK. MCM proteins in DNA replication. Annu Rev Biochem 1999;68:649–86.
[7] Kearsey SE, Maiorano D, Holmes EC, Todorov IT. The role of MCM proteins in the cell cycle control of genome duplication. Bioessays 1996;18:183–90.
[8] Labib K, Tercero JA, Diffley JF. Uninterrupted MCM2-7 function required for DNA replication fork progression. Science 2000;288:1643–7.
[9] Freeman A, Morris LS, Mills AD, Stoeber K, Laskey RA, Williams GH, et al. Minichromosome maintenance proteins as biological markers of dysplasia and malignancy. Clin Cancer Res 1999;5:2121–32.
[10] Stoeber K, Tlsty TD, Happerfield L, Thomas GA, Romanov S, Bobrow L, et al. DNA replication licensing and human cell proliferation. J Cell Sci 2001;114:2027–41.
[11] Williams GH, Romanowski P, Morris L, Madine M, Mills AD, Stoeber K, et al. Improved cervical smear assessment using antibodies against proteins that regulate DNA replication. Proc Natl Acad Sci USA 1998;95:14932–7.
[12] Stoeber K, Swinn R, Prevost AT, de Clive-Lowe P, Halsall I, Dilworth SM, et al. Diagnosis of genito-urinary tract cancer by detection of minichromosome maintenance 5 protein in urine sediments. J Natl Cancer Inst 2002;94:1071–9.
[13] Going JJ, Keith WN, Neilson L, Stoeber K, Stuart RC, Williams GH. Aberrant expression of minichromosome maintenance proteins 2 and 5, and Ki-67 in dysplastic squamous oesophageal epithelium and Barrett's mucosa. Gut 2002;50:373–7.
[14] Gonzalez MA, Pinder SE, Callagy G, Vowler SL, Morris LS, Bird K, et al. Minichromosome maintenance protein 2 is a strong independent prognostic marker in breast cancer. J Clin Oncol 2003;21:4306–13.
[15] Ramnath N, Hernandez FJ, Tan DF, Huberman JA, Natarajan N, Beck AF, et al. MCM2 is an independent predictor of survival in patients with non-small-cell lung cancer. J Clin Oncol 2001;19:4259–66.
[16] Tan DF, Huberman JA, Hyland A, Loewen GM, Brooks JS, Beck AF, et al. MCM2—a promising marker for premalignant lesions of the lung: a cohort study. BMC Cancer 2001;1:6.
[17] Yang J, Ramnath N, Moysich KB, Asch HL, Swede H, Alrawi SJ, et al. Prognostic significance of MCM2, Ki-67 and gelsolin in non-small cell lung cancer. BMC Cancer 2006;6:203.
[18] Hashimoto K, Araki K, Osaki M, Nakamura H, Tomita K, Shimizu E, et al. Ki-67 expression in human lung adenocarcinoma: prognostic implications. Pathobiology 2004;71:193–200.
[19] Ishii M, Hashimoto S, Tsutsumi S, Wada Y, Matsushima K, Kodama T, et al. Direct comparison of GeneChip and SAGE on the quantitative accuracy in transcript profiling analysis. Genomics 2000;68:136–43.
[20] The World Health Organization histological typing of lung tumours. Second ed. Am J Clin Pathol 1982;77:123–136.

[21] American Joint Committee on Cancer. Lung. In: Beahrs OHHD, Hutter RVP, Kennedy BJ, editors. Manual for Staging of Cancer. Philadelphia: Lippincott; 1992.
[22] Mishina T, Dosaka-Akita H, Hommura F, Nishi M, Kojima T, Ogura S, et al. Cyclin E expression, a potential prognostic marker for non-small cell lung cancers. Clin Cancer Res 2000;6:11–6.
[23] Hommura F, Dosaka-Akita H, Mishina T, Nishi M, Kojima T, Hiroumi H, et al. Prognostic significance of p27KIP1 protein and ki-67 growth fraction in non-small cell lung cancers. Clin Cancer Res 2000;6:4073–81.
[24] Ryu S, Holzschuh J, Erhardt S, Ettl AK, Driever W. Depletion of minichromosome maintenance protein 5 in the zebrafish retina causes cell-cycle defect and apoptosis. Proc Natl Acad Sci USA 2005;102:18467–72.
[25] Shima N, Alcaraz A, Liachko I, Buske TR, Andrews CA, Munroe RJ, et al. A viable allele of Mcm4 causes chromosome instability and mammary adenocarcinomas in mice. Nat Genet 2007;39:93–8.
[26] Shreeram S, Sparks A, Lane DP, Blow JJ. Cell type-specific responses of human cells to inhibition of replication licensing. Oncogene 2002;21:6624–32.
[27] Nagai Y, Miyazawa H, Huqun, Tanaka T, Udagawa K, Kato M, et al. Genetic heterogeneity of the epidermal growth factor receptor in non-small cell lung cancer cell lines revealed by a rapid and sensitive detection system, the peptide nucleic acid-locked nucleic acid PCR clamp. Cancer Res 2005;65:7276–82.
[28] Yatabe Y. EGFR mutations and the terminal respiratory unit. Cancer Metastasis Rev 2010;29:23–36.
[29] Yatabe Y, Kosaka T, Takahashi T, Mitsudomi T. EGFR mutation is specific for terminal respiratory unit type adenocarcinoma. Am J Surg Pathol 2005;29:633–9.
[30] Schrader C, Janssen D, Klapper W, Siebmann JU, Meusers P, Brittinger G, et al. Minichromosome maintenance protein 6, a proliferation marker superior to Ki-67 and independent predictor of survival in patients with mantle cell lymphoma. Br J Cancer 2005;93:939–45.
[31] Eward KL, Obermann EC, Shreeram S, Loddo M, Fanshawe T, Williams C, et al. DNA replication licensing in somatic and germ cells. J Cell Sci 2004;117:5875–86.
[32] Kingsbury SR, Loddo M, Fanshawe T, Obermann EC, Prevost AT, Stoeber K, et al. Repression of DNA replication licensing in quiescence is independent of geminin and may define the cell cycle state of progenitor cells. Exp Cell Res 2005;309:56–67.
[33] Ishimi Y, Okayasu I, Kato C, Kwon HJ, Kimura H, Yamada K, et al. Enhanced expression of Mcm proteins in cancer cells derived from uterine cervix. Eur J Biochem 2003;270:1089–101.
[34] Huang XP, Rong TH, Wu QL, Fu JH, Yang H, Zhao JM, et al. MCM4 expression in esophageal cancer from southern China and its clinical significance. J Cancer Res Clin Oncol 2005;131:677–82.
[35] Lei M. The MCM complex: its role in DNA replication and implications for cancer therapy. Curr Cancer Drug Targets 2005;5:365–80.
[36] Fujioka S, Shomori K, Nishihara K, Yamaga K, Nosaka K, Araki K, et al. Expression of minichromosome maintenance 7 (MCM7) in small lung adenocarcinomas (pT1): prognostic implication. Lung Cancer 2009;65:223–9.

^{18}F-Fluorothymidine PET/CT as an early predictor of tumor response to treatment with cetuximab in human lung cancer xenografts

SATOSHI TAKEUCHI[1], SONGJI ZHAO[2,3], YUJI KUGE[4], YAN ZHAO[3], KEN-ICHI NISHIJIMA[3], TOSHIYUKI HATANO[3], YASUSHI SHIMIZU[1], ICHIRO KINOSHITA[1], NAGARA TAMAKI[2] and HIROTOSHI DOSAKA-AKITA[1]

Departments of [1]Medical Oncology, [2]Nuclear Medicine and [3]Tracer Kinetics and Bioanalysis, Graduate School of Medicine, [4]Central Institute of Isotope Science, Hokkaido University, Sapporo, Hokkaido 060-8638, Japan

Received April 26, 2011; Accepted May 17, 2011

DOI: 10.3892/or.2011.1338

Abstract. We investigated whether ^{18}F-fluorothymidine-positron-emission tomography/computed tomography (^{18}F-FLT-PET/CT) is useful for the evaluation of the very early response to anti-epidermal growth factor receptor (EGFR) antibody cetuximab therapy in human lung cancer xenografts. A human tumor xenograft model was established with a human non-small cell lung cancer cell line. The mice were randomly assigned to four groups: tumor growth follow-up, *ex vivo* study, PET/CT imaging and non-treated control. Mice were administered saline as control or cetuximab on day 1. An immunohistochemical study with Ki-67 was performed. Tumor volume treated with cetuximab was kept significantly smaller than control after day 8, although there was no difference on day 3. On day 3, ^{18}F-FLT distribution was higher in the tumor than in other tissues, and was significantly decreased by treatment with cetuximab. On PET/CT imaging, ^{18}F-FLT distribution in the tumor was clearly visualized, and the maximum standardized uptake value (SUV) was significantly decreased after treatment with cetuximab ($p<0.01$). Ki-67 expression was also significantly decreased on day 3 ($p=0.01$). These results suggest that ^{18}F-FLT-PET/CT can be a useful predictor to determine the response to molecular targeted drugs such as cetuximab at an earlier time point than the change of tumor size.

Introduction

Through recent advances in molecular targeted therapy of cancer, applications targeting epidermal growth factor receptor (EGFR) are currently one of the most promising and well advanced in the clinical setting. EGFR is a protein tyrosine kinase that plays a crucial role in signal transduction pathways, regulating key cellular functions such as proliferation, angiogenesis, metastasis, and evasion of apoptosis (1,2). EGFR targeting therapy is promising for non-small cell lung cancers (NSCLCs). The EGFR tyrosine kinase inhibitors (EGFR-TKIs) erlotinib (3) and gefitinib (4,5) are established treatments for patients with advanced NSCLCs. Anti-EGFR antibody drugs have also been developed. Cetuximab, a chimeric monoclonal antibody targeting EGFR, has recently been used for treatment of patients with advanced NSCLC in a phase III study (6).

In general, molecular targeted drugs targeting EGFR are not only more expensive than commonly used cytotoxic agents, but they may also cause unique side effects, such as dermatologic reactions. To use molecular targeted drugs effectively, it is necessary to develop early and accurate evaluation modalities for the tumor response. The X-ray computed tomography (CT) and magnetic resonance imaging (MRI) have commonly been used to evaluate the anti-tumor effect of these cytotoxic and molecular targeted drugs by measuring tumor size. However, these anatomical imaging techniques have limited value due to requiring a relatively long time to obtain tumor size shrinkage with successful drug therapy. Thus, patients may have to endure side effects (7) and high medical costs (8) during periods of desperate treatment. In addition, evaluation based on sequential measurement of tumor size may not accurately reflect viable tumor cells because of the presence of necrotic or fibrotic tissue (9).

Nuclear imaging, including positron emission tomography (PET), has recently been used for treatment evaluation, in addition to conventional methods such as CT and MRI. It can provide information about pathophysiological function, while CT and MRI evaluations are based on sequential measurements of tumor size. The thymidine analog 3'-deoxy-3'-^{18}F-fluorothymidine (^{18}F-FLT) has been developed as a PET tracer to image proliferation *in vivo* (10). ^{18}F-FLT uptake has been shown to reflect the activity of thymidine kinase-1 (TK1), an enzyme expressed during the DNA synthesis phase of the cell cycle. TK1 activity is high in proliferating cells and low in

Correspondence to: Dr Yuji Kuge, Central Institute of Isotope Science, Hokkaido University, North 15, West 7, Kita-ku, Sapporo, Hokkaido 060-8638, Japan
E-mail: kuge@ric.hokudai.ac.jp

Key words: ^{18}F-fluorothymidine, cetuximab, lung cancer, PET/CT

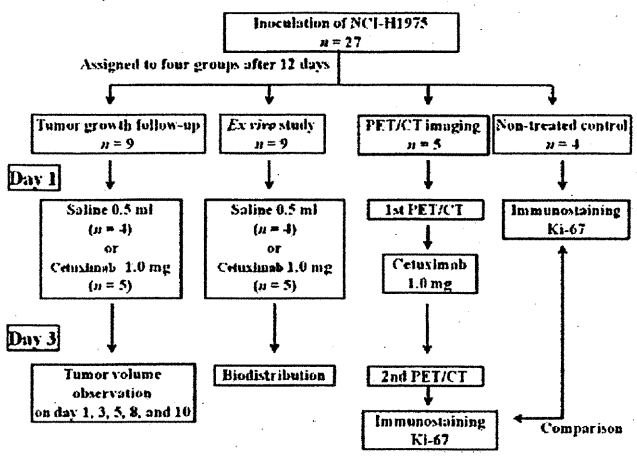

Figure 1. Experimental protocols of this study. Twelve days after inoculation of NCI-H1975 cells, mice were assigned randomly to four groups: tumor growth follow-up, *ex vivo* study, PET/CT imaging, and non-treated control groups. In the tumor growth follow-up and *ex vivo* study groups, the mice were further assigned to be administered saline or cetuximab. In the *ex vivo* study group, mice were sacrificed for a biodistribution study on day 3. In the PET/CT imaging group, mice were imaged by PET/CT pre-treatment with cetuximab on day 1. The same mice were imaged again with the same procedure post-treatment on day 3. Tumor cell proliferative activity (Ki-67 labeling index) was determined by immunohistochemistry. In the non-treated group, the Ki-67 labeling index of the tumor was determined as a control value and compared with that in the PET/CT imaging group.

dormant cells. Owing to the phosphorylation of FLT by TK1, negatively charged FLT monophosphate is formed, resulting in intracellular trapping and accumulation of radioactivity (11). Thus, this tracer is retained in proliferating cells through the activity of thymidine kinase. Measurement of tumor proliferative activity by ^{18}F-FLT-PET/CT may be a way to provide an early and accurate assessment of the response to therapy with molecular targeted drugs (12).

The purpose of this study was to determine whether ^{18}F-FLT-PET/CT is useful to evaluate the response to anti-EGFR antibody cetuximab therapy at very early time points in human lung cancer xenografts.

Materials and methods

Cell line. The human non-small cell lung cancer cell line NCI-H1975 (American Type Culture Collection, Manassas, VA, USA) was cultured in RPMI-1640 medium (Invitrogen Life Technologies, Inc., Carlsbad, CA, USA) supplemented with 10% fetal bovine serum (FBS) and 0.03% glutamine at 37˚C in an atmosphere of 5% CO_2. NCI-H1975 cells contain both the EGFR-TKI-sensitizing L858R and the resistant T790M point mutations (13).

Animal studies. All experimental protocols were approved by the Laboratory Animal Care and Use Committee of Hokkaido University. Nine-week-old male BALB/c athymic nude mice (supplied by Japan SLC, Inc., Hamamatsu, Japan) were used in all experiments. A human tumor xenograft model was established using this cell line ($5x10^6$ cells/0.1 ml) by s.c. inoculation into the right flank of the mice. Twelve days after inoculation (when the tumors reached 7-10 mm in diameter) (14), the mice were randomly assigned to four groups: tumor growth follow-up (n=9), *ex vivo* study (n=9), PET/CT imaging (n=5), and non-treated control (n=4) groups. Fig. 1 shows the experimental protocols of this study.

In the tumor growth follow-up and *ex vivo* groups, the mice were further assigned to be administered saline 0.5 ml/mouse as control or cetuximab 1.0 mg/0.5 ml/mouse given intraperitoneally. The monoclonal anti-EGFR antibody cetuximab (IMC-C225; Erbitux) was kindly provided by Merck KGaA (Darmstadt, Germany). In the tumor growth follow-up group, tumor sizes were measured by caliper on days 3, 5, 8, and 10 after the treatment on day 1. Tumor volume was calculated by the formula: $\pi/6$ x larger diameter x (smaller diameter)^2. In the *ex vivo* study group, mice were anesthetized with isoflurane inhalation and injected with 7.4 MBq of ^{18}F-FLT in the tail vein. After 90 min, these mice were sacrificed, and the tumor and other organs were excised. The tissue and blood samples were weighed, and radioactivity of tracers in each sample was determined using a gamma-counter (1480 Wizard 3, Wallac Oy, Turku, Finland). Tracer uptake in the tissue was expressed as the percentage of injected dose (ID) per gram of tissue after being normalized to the animal's weight (%ID/g) x kg. Uptake was calculated in the tumor and normal organs, including blood, plasma, muscle, heart, lung, spleen, liver, pancreas, stomach, small intestine, colon, kidney, skin, brown fat and brain. In the PET/CT imaging group, mice were imaged by a small animal PET/CT for 20 min pre-treatment before administration of cetuximab on day 1. The same mice were again imaged with the same procedure post-treatment with cetuximab on day 3. Tumor sizes were measured before each PET/CT imaging session. In the non-treated control group, the tumor cell proliferative activity (Ki-67 labeling index) was determined as the control value and compared with that of the PET/CT imaging group.

^{18}F-FLT-PET/CT studies. In the PET/CT imaging group (n=5), the mice were anesthetized with isoflurane inhalation and injected with 7.4 MBq of ^{18}F-FLT into the tail vein. ^{18}F-FLT was synthesized and obtained from the Hokkaido University Hospital Cyclotron facility. It was synthesized using a modification of a previously published procedure (15). The mice were placed in a small animal PET/CT scanner (Inveon; Siemens Medical Solutions USA Inc., Knoxville, TN) in a supine position 60 min after the injection of ^{18}F-FLT. PET and CT scans were carried out for 20 and 7 min, respectively for image capture. The mice were kept using cotton bedding of our own making to maintain body temperature and anesthetized with 1.0-1.5% isoflurane inhalation during the PET/CT imaging. Following the second PET/CT imaging (90 min after the injection of ^{18}F-FLT), the mice were sacrificed, and tumor tissues were excised for immunohistochemical staining. The data were reconstructed and corrected for attenuation and scattering using 2D filtered back-projection (FBP). The image matrix was 256 x 256 x 159, resulting in a voxel size of 0.385 x 0.385 x 0.796 mm. Images were analyzed quantitatively by drawing volumes of interest centered over the tumor without correction for partial volume effects. The standardized uptake value (SUV) was calculated using the single maximum pixel count within the region of interest and normalized to the injected dose and mouse body weight. SUVmax denotes the maximum SUV value within the

tumor region of interest (ROI). Using tissue samples from the tumors, formalin-fixed, paraffin-embedded specimens were prepared for subsequent histological staining.

Pathological study. Formalin-fixed, paraffin-embedded, 3-μm thick sections of tumor were used for immunohistochemical staining. The labeled streptavidin biotin method was used after deparaffinization. Immunohistochemical staining of nuclear antigen Ki-67 was performed as a tumor cell proliferation marker. The primary antibody used was a mouse monoclonal antibody for Ki-67, clone MIB-1 (Dako, Carpinteria, CA). Tumor cells were considered positive only when clear nuclear staining was seen. All nuclei with homogeneous granular staining or multiple speckled staining were counted as positive, regardless of the staining intensity. Cells with cytoplasmic staining were excluded (16). The Ki-67 labeling index was defined as the percentage of positive cells by counting cell numbers in the entire field of the tumor.

Statistical analysis. All values are expressed as means ± SD (standard deviation). Two-way repeated measures analysis of variance (ANOVA) and the unpaired Student's t-test were used to compare tumor volume sequentially for the tumor growth follow-up group. The unpaired Student's t-test was used to compare the biodistribution of ^{18}F-FLT between the two treatment groups. Paired Student's t-tests were used to compare the differences between different time points within one treatment group. A p-value of <0.05 was considered significant. Statistical analysis was performed using SPSS 14.0 for Windows (SPSS Inc., Chicago, IL).

Results

Tumor volume change. Tumor volume change in the tumor growth follow-up group is shown in Fig. 2. The mice were treated by saline or cetuximab on day 1. The tumor volumes of the control group and cetuximab-treated groups were 150.9±38.6 and 131.4±45.9 mm^3, respectively, on day 3. Although there was no difference in the tumor volume between these two groups on day 3, the tumor grew rapidly in the control group. A significant difference was observed on day 8. The tumor volumes of the control and cetuximab-treated groups were 381.4±99.6 and 140.3±37.9 mm^3, respectively ($p<0.01$). The difference became more obvious on day 10 ($p<0.01$). On the other hand, tumors were maintained almost within the same size in the cetuximab-treated group. The tumor volume of the cetuximab-treated groups was 117.5±46.9 mm^3 on day 1, and was kept 172.8±61.3 mm^3 even on day 10. This indicated that the dose of cetuximab used was adequate to suppress tumor growth, and that cetuximab treatment had enough efficacy to suppress tumor growth. Considering this result, an *ex vivo* study and ^{18}F-FLT-PET/CT imaging were performed on day 3 for early evaluation of therapy response.

Biodistribution of ^{18}F-FLT. The biodistribution of ^{18}F-FLT in the *ex vivo* study group on day 3 is shown in Fig. 3. The radioactivity was higher in the tumor than in other organs in the control group. A significant difference in the biodistribution of ^{18}F-FLT in the tumor was observed between the control and cetuximab-treated groups. Biodistributions in the control

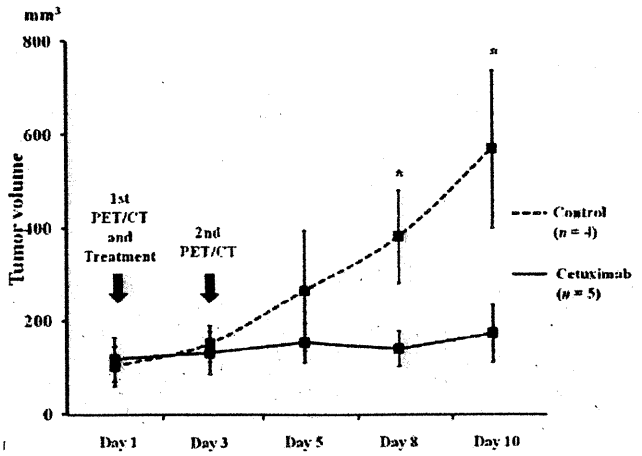

Figure 2. Change in tumor volume in the tumor growth follow-up group. Mice were treated by saline or cetuximab on day 1. There was no obvious difference in size between the two groups until day 3. Since the tumors began to grow rapidly in the control group, significant differences were seen from day 8 (*p<0.01). Tumors were maintained almost within the same size in the cetuximab-treated group.

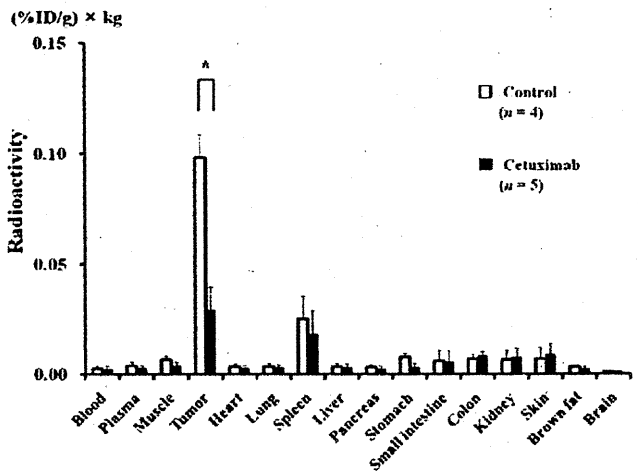

Figure 3. Biodistribution of ^{18}F-FLT in the *ex vivo* study group on day 3. The ^{18}F-FLT uptake was higher in tumor than in other normal organs. The uptake was significantly decreased in the cetuximab-treated group compared with the control group (*p<0.001).

and cetuximab-treated groups were 0.098±0.005 (%ID/g) x kg and 0.029±0.010 (%ID/g) x kg, respectively ($p<0.001$). ^{18}F-FLT uptake was particularly high in the tumors, and it was decreased by cetuximab treatment as early as day 3. This result indicates that ^{18}F-FLT may be promising to assess the early response to therapy.

^{18}F-FLT-PET/CT image. The *in vivo* imaging by ^{18}F-FLT-PET/CT was performed on day 1 before treatment with cetuximab and then again for the same mice on day 3. A representative image of the first ^{18}F-FLT-PET/CT before treatment is shown in Fig. 4A. Since the high uptake of ^{18}F-FLT was seen only in the tumor, it can be clearly visualized with PET/CT before treatment with cetuximab. Fig. 4B shows the image of the second ^{18}F-FLT-PET/CT after treatment with cetuximab on

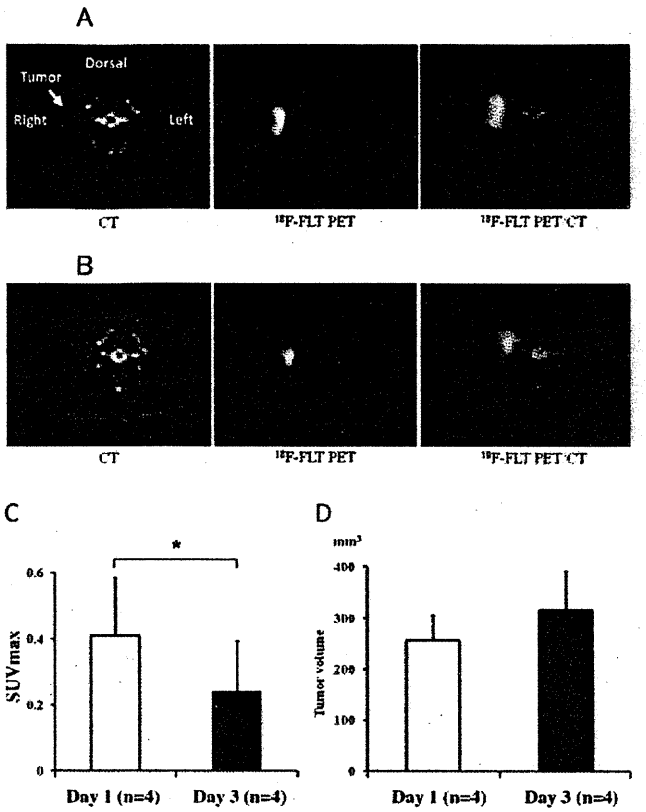

Figure 4. CT, ^{18}F-FLT PET and ^{18}F-FLT-PET/CT images and the mazimum standardized uptake value (SUVmax). (A) Representative images on day 1 before treatment, and on day 3 after treatment with cetuximab (B). Tumor is seen on the right flank of the animal. The high FLT uptake is seen only in the tumor. The uptake is decreased after treatment with cetuximab as early as day 3 (*p<0.01). (C) The SUVmax from tumor ROIs is shown. There is a significant difference between day 1 before treatment and on day 3 after treatment with cetuximab. (D) Tumor volume in the ^{18}F-FLT-PET/CT imaging group is shown. There is no significant difference in tumor volume between before and after treatment with cetuximab (p=0.11).

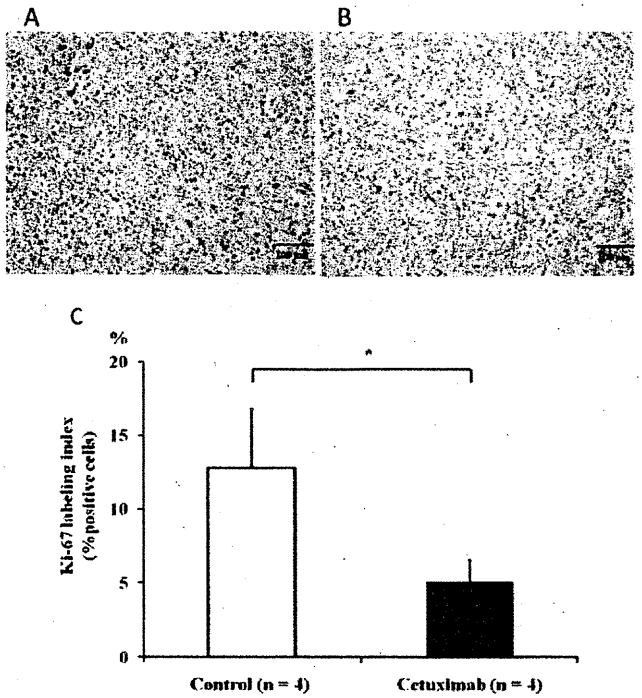

Figure 5. Representative immunohistochemical staining of Ki-67 and the Ki-67 labeling index on day 3. (A) Ki-67 staining in the non-treated control group as a control. (B) Ki-67 staining in the PET/CT imaging group post-treatment with cetuximab. Scale bar, 100 μm. (C) The Ki-67 labeling index shows a significant difference between day 1 before treatment and day 3 after treatment with cetuximab (*p=0.01).

day 3. Decreased ^{18}F-FLT uptake after treatment was visualized. SUVmax values from tumor ROIs were obtained from each ^{18}F-FLT-PET/CT (Fig. 4C). There was a significant difference between day 1 before treatment and day 3 after treatment with cetuximab (0.41±0.17 before treatment on day 1 and 0.24±0.15 after treatment on day 3; p<0.01). However, in this ^{18}F-FLT-PET/CT imaging group, there was no significant change in tumor volume between before and after cetuximab treatment (257.0±49.3 mm^3 before treatment on day 1 and 315.5±77.1 mm^3 after treatment on day 3; p=0.11) (Fig. 4D). These results show that ^{18}F-FLT-PET/CT could visualize the change in tumor proliferation at a very early time point even without a significant change in tumor size.

Pathological study. Since ^{18}F-FLT-PET/CT visualized the change in tumor proliferation between before and after treatment with cetuximab, a pathological study was performed using tumor samples of this PET/CT imaging group. Hence, the non-treated control group was used as the control. Representative immunohistochemical staining for Ki-67 in the non-treated control group is shown in Fig. 5A as a control on day 1. Fig. 5B shows Ki-67 staining in the PET/CT imaging group post-treatment with cetuximab on day 3. Two days after the administration of cetuximab, there was a decrease in Ki-67-positive tumor cells. There was a significant difference in the Ki-67 labeling index between them (12.8±4.0% in the non-treated control group on day 1 vs. 5.0±1.5% in the PET/CT imaging group on day 3; p=0.01) (Fig. 5C). This result indicates that tumor proliferation was suppressed by cetuximab treatment as early as day 3, and this was consistent with the result of ^{18}F-FLT-PET/CT imaging.

Discussion

The present study demonstrated that ^{18}F-FLT-PET/CT may evaluate the therapeutic effect earlier than morphological measurement on CT in human cancer cell line xenografts, and that such a method could be useful to evaluate the effects of molecular targeted drugs such as cetuximab. Although there was no difference in tumor volume between the control and cetuximab-treated groups on day 3, tumor began to grow rapidly in the control group after day 3. On the other hand, the tumor was maintained almost within the same size in the cetuximab-treated group. Early changes in tumor proliferation could be visualized by non-invasive ^{18}F-FLT-PET/CT imaging, even when significant changes in tumor size were still not seen. The early change in tumor proliferation activity was confirmed by a pathological study using the Ki-67 labeling index. Thus, measurement of tumor proliferative activity by ^{18}F-FLT-PET/CT may be a way to provide an early and accurate assessment of the response to therapy with molecular targeted drugs for cancer.

Cetuximab has activity in various types of cancer, including head and neck cancer, colorectal cancer, and non-small cell lung cancer (6,17,18). Early and accurate evaluation methods for using cetuximab effectively are urgently required. Examining the K-ras mutation in advance before treatment with cetuximab is one solution (19). Patients bearing tumors with the mutated K-ras gene do not benefit from cetuximab in colorectal cancer. In contrast with colorectal cancer, the significance of K-ras mutation in non-small cell lung cancer has not yet been well clarified, even in the latest phase III study (6,20). Cetuximab-induced skin toxicity is also a predictive marker (7) and helps identify those patients for whom cetuximab is effective. The appearance of skin toxicities, however, is too variable and not a direct predictor of tumor response itself. As for nuclear imaging, the effectiveness of ^{18}F-FLT has attracted increasing interest (10,21,22).

A recent study showed that monotherapy with cetuximab was not effective in patients with advanced NSCLC who received prior EGFR-TKI treatment (23). However, in the present study, we used the human non-small cell lung cancer cell line NCI-H1975 which contains both the EGFR-TKI-sensitizing L858R and the resistant T790M point mutations (13). A previous study showed that cetuximab had antitumor activity even in this mutated cell line (24). Hence, this xenograft model using NCI-H1975 is suitable and reasonable to evaluate the early response to cetuximab therapy.

Since ^{18}F-FLT-PET/CT reflects the proliferation of tumor cells, this method is more suitable for detecting the early therapeutic effect compared with conventional modalities such as CT and MRI, which are based on sequential measurements of tumor size. This present study showed the effectiveness of ^{18}F-FLT-PET/CT in the evaluation of the therapeutic effect of cetuximab in human lung cancer xenografts at an earlier time point (day 3) than the change of tumor size. As molecular targeted drugs are used for patients with advanced-stage cancer, it is very important to know the therapeutic effect as early as possible. If the therapeutic effect can be predicted at a very early time point, it will be possible to select the clinically optimal treatment and reduce toxicity and medical costs in advance. To our knowledge, several investigators recently used ^{18}F-FLT-PET to evaluate treatment response in animal models following EGFR targeted therapy such as erlotinib and cetuximab. However, those studies performed ^{18}F-FLT-PET at later timing than our study (25), and did not use lung cancer cell line (26) or cetuximab (27).

Whether ^{18}F-FLT-PET/CT on day 3 is the best timing for early treatment evaluation remains unclear. Herrmann *et al* reported that ^{18}F-FLT-PET imaging 2 days after administration of cyclophosphamide-adriamycin-vincristine-prednisone chemotherapy with rituximab immunotherapy showed an early decrease in ^{18}F-FLT uptake in lymphoma patients, while there was no reduction in ^{18}F-FLT uptake after rituximab alone (28), though both cetuximab and rituximab are a type of the same chimeric antibody. Atkinson *et al* reported that ^{18}F-FLT-PET imaging could detect tumor response to anti-EGFR treatment using cetuximab as well as erlotinib (25). Their ^{18}F-FLT PET imaging was performed 7 days after treatment. Considering these results, the best timing for early evaluation may depend on the kind of disease and the drugs used. In any case, ^{18}F-FLT-PET/CT may be a potent modality for earlier response evaluation than conventional modalities such as CT and MRI. However, it remains to be clarified whether ^{18}F-FLT is useful to assess the early therapeutic effect for other malignant tumors, and whether ^{18}F-FLT can be useful when other molecular targeted drugs, such as anti-angiogenesis drugs, are used.

It should be noted that cetuximab has an immune-mediated antitumor mechanism called antibody-dependent cell-mediated cytotoxicity (ADCC). ADCC is supposed to contribute to the activity of cetuximab (29). In the present study, the tumor model was established in immune-deficient mice (BALB/c athymic nude mouse) that lack function of a T-cell component. Hence, the efficacy of cetuximab might be less effective than it should be. Although further investigation is needed to apply our result to immune-competent mice or humans, genetically engineered mouse models have been proven to be a powerful tool for elucidation of the biological processes and pathophysiological alterations that occur in human disease (9).

^{18}F-fluorodeoxyglucose (FDG) is the most widely used tracer for tumor imaging with PET and can image viable tumor cells by reflecting glucose metabolism. Avril *et al* reported a significant correlation between ^{18}F-FDG uptake and proliferative activity in breast cancer (30), but the correlation coefficient was low (0.41). On the other hand, Brepoels *et al* reported that ^{18}F-FLT is a more accurate measurement of tumor response than ^{18}F-FDG after the administration of cyclophosphamide (31). It is well known that ^{18}F-FDG is not tumor specific, since its uptake occurs in inflammatory lesions where glucose is utilized (32). ^{18}F-FDG-PET may not clearly distinguish between residual disease and post-treatment inflammation (33). ^{18}F-FDG shows considerable accumulation in macrophages and granulation tissues (34). These characteristics of ^{18}F-FDG suggest that careful assessment is needed when using ^{18}F-FDG to evaluate treatment, though further studies, including comparative studies between ^{18}F-FLT and ^{18}F-FDG, and also with various tumor biomarkers are necessary to demonstrate the advantages of ^{18}F-FLT-PET. Although we injected ^{18}F-FDG into this xenograft model, tracer uptake in the tumor was not high compared to other organs, and was not decreased by cetuximab treatment (data not shown).

In conclusion, the results of this study suggest that ^{18}F-FLT-PET/CT can be useful for evaluating the response to molecular targeted drugs such as cetuximab at an earlier time point than the evaluation of tumor size in human lung cancer cell line xenografts. In the future, clinical studies evaluating ^{18}F-FLT-PET/CT as an early predictor of tumor response to anti-EGFR antibody drugs will be required. In the clinical setting, ^{18}F-FLT-PET/CT is expected to optimize clinical outcomes and reduce exposure to an ineffective treatment. It is also expected to avoid toxicity, to decrease duration of treatment, and to reduce medical costs in advance.

Acknowledgements

This study was performed through special coordination funds for promoting science and technology, provided by the Ministry of Education, Culture, Sports, Science, and Technology of the Japanese Government. This study was also supported in part by grants-in-aid for Scientific Research from the Japan Society for the Promotion of Science. The authors would like to thank

the staff members of the Department of Nuclear Medicine, Department of Medical Oncology, Central Institute of Isotope Science and Institute for Animal Experimentation, Hokkaido University, and Hokkaido University Hospital for supporting this study.

References

1. Wieduwilt MJ and Moasser MM: The epidermal growth factor receptor family: biology driving targeted therapeutics. Cell Mol Life Sci 65: 1566-1584, 2008.
2. Dassonville O, Bozec A, Fischel JL and Milano G: EGFR targeting therapies: monoclonal antibodies versus tyrosine kinase inhibitors. Similarities and differences. Crit Rev Oncol Hematol 62: 53-61, 2007.
3. Shepherd FA, Rodrigues Pereira J, Ciuleanu T, *et al*: Erlotinib in previously treated non-small cell lung cancer. N Engl J Med 353: 123-132, 2005.
4. Mitsudomi T, Morita S, Yatabe Y, *et al*: Gefitinib versus cisplatin plus docetaxel in patients with non-small cell lung cancer harbouring mutations of the epidermal growth factor receptor (WJTOG3405): an open label, randomised phase 3 trial. Lancet Oncol 11: 121-128, 2010.
5. Maemondo M, Inoue A, Kobayashi K, *et al*: Gefitinib or chemotherapy for non-small cell lung cancer with mutated EGFR. N Engl J Med 362: 2380-2388, 2010.
6. Pirker R, Pereira JR, Szczesna A, *et al*: Cetuximab plus chemotherapy in patients with advanced non-small cell lung cancer (FLEX): an open-label randomised phase III trial. Lancet 373: 1525-1531, 2009.
7. Lynch TJ Jr, Kim ES, Eaby B, Garey J, West DP and Lacouture ME: Epidermal growth factor receptor inhibitor-associated cutaneous toxicities: an evolving paradigm in clinical management. Oncologist 12: 610-621, 2007.
8. Mittmann N, Au HJ, Tu D, *et al*: Prospective cost-effectiveness analysis of cetuximab in metastatic colorectal cancer: evaluation of National Cancer Institute of Canada Clinical Trials Group CO.17 trial. J Natl Cancer Inst 101: 1182-1192, 2009.
9. Spaepen K, Stroobants S, Dupont P, *et al*: [(18)F]FDG PET monitoring of tumour response to chemotherapy: does [(18)F] FDG uptake correlate with the viable tumour cell fraction? Eur J Nucl Med Mol Imaging 30: 682-688, 2003.
10. Shields AF, Grierson JR, Dohmen BM, *et al*: Imaging proliferation in vivo with [F-18]FLT and positron emission tomography. Nat Med 4: 1334-1336, 1998.
11. Toyohara J, Waki A, Takamatsu S, Yonekura Y, Magata Y and Fujibayashi Y: Basis of FLT as a cell proliferation marker: comparative uptake studies with [3H]thymidine and [3H]arabinothymidine, and cell-analysis in 22 asynchronously growing tumor cell lines. Nucl Med Biol 29: 281-287, 2002.
12. Yang DJ, Kim EE and Inoue T: Targeted molecular imaging in oncology. Ann Nucl Med 20: 1-11, 2006.
13. Pao W, Miller VA, Politi KA, *et al*: Acquired resistance of lung adenocarcinomas to gefitinib or erlotinib is associated with a second mutation in the EGFR kinase domain. PLoS Med 2: e73, 2005.
14. Zhao S, Takeuchi S, Kuge Y, *et al*: FLT PET can ealrly predict antiproliferative response to anti-EGFR molecular targeting therapy (cetuximab) in human lung cancer xenograft. J Nucl Med 51 (Suppl 2): 399, 2010.
15. Oh SJ, Mosdzianowski C, Chi DY, *et al*: Fully automated synthesis system of 3'-deoxy-3'-[18F]fluorothymidine. Nucl Med Biol 31: 803-809, 2004.
16. Spyratos F, Ferrero-Pous M, Trassard M, *et al*: Correlation between MIB-1 and other proliferation markers: clinical implications of the MIB-1 cut-off value. Cancer 94: 2151-2159, 2002.
17. Bonner JA, Harari PM, Giralt J, *et al*: Radiotherapy plus cetuximab for squamous-cell carcinoma of the head and neck. N Engl J Med 354: 567-578, 2006.
18. Goldberg RM, Rothenberg ML, Van Cutsem E, *et al*: The continuum of care: a paradigm for the management of metastatic colorectal cancer. Oncologist 12: 38-50, 2007.
19. Karapetis CS, Khambata-Ford S, Jonker DJ, *et al*: K-ras mutations and benefit from cetuximab in advanced colorectal cancer. N Engl J Med 359: 1757-1765, 2008.
20. Khambata-Ford S, Harbison CT, Hart LL, *et al*: Analysis of potential predictive markers of cetuximab benefit in BMS099, a phase III study of cetuximab and first-line taxane/carboplatin in advanced non-small cell lung cancer. J Clin Oncol 28: 918-927, 2010.
21. Vesselle H, Grierson J, Muzi M, *et al*: In vivo validation of 3'deoxy-3'-[(18)F]fluorothymidine ([(18)F]FLT) as a proliferation imaging tracer in humans: correlation of [(18)F]FLT uptake by positron emission tomography with Ki-67 immunohistochemistry and flow cytometry in human lung tumors. Clin Cancer Res 8: 3315-3323, 2002.
22. Salskov A, Tammisetti VS, Grierson J and Vesselle H: FLT: measuring tumor cell proliferation in vivo with positron emission tomography and 3'-deoxy-3'-[18F]fluorothymidine. Semin Nucl Med 37: 429-439, 2007.
23. Neal JW, Heist RS, Fidias P, *et al*: Cetuximab monotherapy in patients with advanced non-small cell lung cancer after prior epidermal growth factor receptor tyrosine kinase inhibitor therapy. J Thorac Oncol 5: 1855-1858, 2010.
24. Steiner P, Joynes C, Bassi R, *et al*: Tumor growth inhibition with cetuximab and chemotherapy in non-small cell lung cancer xenografts expressing wild-type and mutated epidermal growth factor receptor. Clin Cancer Res 13: 1540-1551, 2007.
25. Atkinson DM, Clarke MJ, Mladek AC, *et al*: Using fluorodeoxythymidine to monitor anti-EGFR inhibitor therapy in squamous cell carcinoma xenografts. Head Neck 30: 790-799, 2008.
26. Manning HC, Merchant NB, Foutch AC, *et al*: Molecular imaging of therapeutic response to epidermal growth factor receptor blockade in colorectal cancer. Clin Cancer Res 14: 7413-7422, 2008.
27. Ullrich RT, Zander T, Neumaier B, *et al*: Early detection of erlotinib treatment response in NSCLC by 3'-deoxy-3'-[F]-fluoro-L-thymidine ([F]FLT) positron emission tomography (PET). PLoS One 3: e3908, 2008.
28. Herrmann K, Wieder HA, Buck AK, *et al*: Early response assessment using 3'-deoxy-3'-[18F]fluorothymidine-positron emission tomography in high-grade non-Hodgkin's lymphoma. Clin Cancer Res 13: 3552-3558, 2007.
29. Mendelsohn J and Baselga J: The EGF receptor family as targets for cancer therapy. Oncogene 19: 6550-6565, 2000.
30. Avril N, Menzel M, Dose J, *et al*: Glucose metabolism of breast cancer assessed by 18F-FDG PET: histologic and immunohistochemical tissue analysis. J Nucl Med 42: 9-16, 2001.
31. Brepoels L, Stroobants S, Verhoef G, De Groot T, Mortelmans L and De Wolf-Peeters C: (18)F-FDG and (18)F-FLT uptake early after cyclophosphamide and mTOR inhibition in an experimental lymphoma model. J Nucl Med 50: 1102-1109, 2009.
32. Yamada S, Kubota K, Kubota R, Ido T and Tamahashi N: High accumulation of fluorine-18-fluorodeoxyglucose in turpentine-induced inflammatory tissue. J Nucl Med 36: 1301-1306, 1995.
33. Shreve P, Anzai Y and Wahl R: Pitfalls in oncologic diagnosis with FDG PET imaging: physiologic and benign variants. Radiographics 19: 61, 1999.
34. Kubota R, Yamada S, Kubota K, Ishiwata K, Tamahashi N and Ido T: Intratumoral distribution of fluorine-18-fluorodeoxyglucose in vivo: high accumulation in macrophages and granulation tissues studied by microautoradiography. J Nucl Med 33: 1972-1980, 1992.

ARTICLE IN PRESS

EUROPEAN JOURNAL OF CANCER XXX (2011) XXX–XXX

Available at www.sciencedirect.com

SciVerse ScienceDirect

journal homepage: www.ejconline.com

A multi-institutional phase II trial of consolidation S-1 after concurrent chemoradiotherapy with cisplatin and vinorelbine for locally advanced non-small cell lung cancer

Tomoya Kawaguchi [a,*], *Minoru Takada* [b], *Masahiko Ando* [c], *Kyoichi Okishio* [a], *Shinji Atagi* [a], *Yuka Fujita* [d], *Yoshio Tomizawa* [e], *Kenji Hayashihara* [f], *Yoshio Okano* [g], *Fumiaki Takahashi* [h], *Ryusei Saito* [e], *Akihide Matsumura* [a], *Atsuhisa Tamura* [i]

[a] National Hospital Organization, Kinki-Chuo Chest Medical Center, 1180 Nagasone-cho, Kita-ku, Sakai, Osaka 591-8555, Japan
[b] Kinki University Sakai Hospital, 2-7-2 Harayamadai, Minami-ku, Sakai, Osaka 591-0132, Japan
[c] Kyoto University, Yoshida-Honmachi, Sakyo-ku, Kyoto 606-8501, Japan
[d] NHO Asahikawa Medical Center, 7-4048 Hanasakicho, Asahikawa, Hokkaido 070-0901, Japan
[e] NHO Nishi-Gunma Hospital, 2854 Kanai Shibukawa, Gunma 377-0027, Japan
[f] NHO Ibaraki-higashi Hospital, 825 Terunuma, Nakagun Tokaimura, Ibaraki 319-1113, Japan
[g] NHO Kochi Hospital, 1-2-25 Asakuranishimachi, Kochi, Kochi 780-8077, Japan
[h] Kitazato University, 1-15-1 Kitazato, Sagamihara, Minami-ku, Kanagawa 252-0329, Japan
[i] NHO Tokyo Hospital, 3-1-1 Takeoka, Kiyose, Tokyo 204-002, Japan

ARTICLE INFO

Article history:
Available online xxxx

Keywords:
Chemoradiotherpay
Non-small cell lung cancer
Consolidation
S-1
Japan National Hospital Organization Study Group for Lung Cancer

ABSTRACT

Aim: To evaluate the efficacy and feasibility of the consolidation therapy of the oral fluoropyrimidine agent S-1 after concurrent chemoradiotherapy for unresectable stage III non-small cell lung cancer (NSCLC).

Methods: Eligible patients had unresectable stage III NSCLC with performance status of 0 or 1. Chemoradiotherapy at a total dose of 60 Gy consisted of cisplatin (80 mg/m^2) on days 1 and 29, vinorelbine (20 mg/m^2) on days 1, 8, 29 and 36. Sequential consolidation S-1 therapy was commenced at a dose of 80–120 mg twice daily on day 57 with two cycles of 4 weeks administration and 2 weeks withdrawal.

Results: Of the 66 patients, 65 were evaluated. Chemoradiotherapy was completed in 57 (87.7%) patients, and S-1 consolidation therapy was administered in 45 (69.2%) and completed in 31 (47.6%). Grade 3 pneumonitis developed in three patients with one dying of it. The response rate was 61.5% (95% confidence interval [CI], 48.6–73.3%). The median progression-free survival was 10.2 (95% CI, 8.6–13.7) months and median survival time 21.8 (95% CI, 15.6–27.6) months. The 1- and 3-year survival rates were 73.9% and 34.0%, respectively.

Conclusions: Chemoradiotherapy with cisplatin and vinorelbine followed by S-1 consolidation demonstrated a reasonable overall survival in patients with stage III NSCLC. However, less than half of the patients completed this regimen, and the additional effect of S-1 was marginal compared with historical control.

Conclusions: We concluded that chemoradiotherapy alone is still the recommended standard treatment for patients.

* *Corresponding author:* Address: Department of Internal Medicine, National Hospital Organization, Kinki-Chuo Chest Medical Center, 1180 Nagasone-cho, Kita-ku, Sakai, Osaka 591-8555, Japan. Tel.: +81 72 252 3021; fax: +81 72 251 1372.
E-mail address: t-kawaguchi@kch.hosp.go.jp (T. Kawaguchi).

0959-8049/$ - see front matter © 2011 Elsevier Ltd. All rights reserved.
doi:10.1016/j.ejca.2011.11.020

Please cite this article in press as: Kawaguchi T et al., A multi-institutional phase II trial of consolidation S-1 after concurrent chemoradiotherapy with cisplatin and vinorelbine for locally advanced non-small cell lung cancer, *Eur J Cancer* (2011), doi:10.1016/j.ejca.2011.11.020